Chemical Science

ROYAL SOCIETY OF CHEMISTRY

PERSPECTIVE

View Article Online
View Journal | View Issue

Cite this: *Chem. Sci.*, 2024, **15**, 6200

All publication charges for this article have been paid for by the Royal Society of Chemistry

Received 4th January 2024
Accepted 20th March 2024

DOI: 10.1039/d4sc00070f

rsc.li/chemical-science

Opportunities and challenges for plastic depolymerization by biomimetic catalysis

Yanfen Wu,† Qikun Hu,† Yizhen Che† and Zhiqiang Niu *

Plastic waste has imposed significant burdens on the environment. Chemical recycling allows for repeated regeneration of plastics without deterioration in quality, but often requires harsh reaction conditions, thus being environmentally unfriendly. Enzymatic catalysis offers a promising solution for recycling under mild conditions, but it faces inherent limitations such as poor stability, high cost, and narrow substrate applicability. Biomimetic catalysis may provide a new avenue by combining high enzyme-like activity with the stability of inorganic materials. Biomimetic catalysis has demonstrated great potential in biomass conversion and has recently shown promising progress in plastic degradation. This perspective discusses biomimetic catalysis for plastic degradation from two perspectives: the imitation of the active centers and the imitation of the substrate-binding clefts. Given the chemical similarity between biomass and plastics, relevant work is also included in the discussion to draw inspiration. We conclude this perspective by highlighting the challenges and opportunities in achieving sustainable plastic recycling *via* a biomimetic approach.

1. Introduction

The exponential growth of plastic production and mismanagement of plastic waste over the past few decades have caused escalating concerns across the globe.[1–3] To mitigate the environmental impact of plastic waste, it is imperative to develop plastic recycling approaches beyond landfill and incineration. While mechanical recycling has been used for recovery of thermoplastics, the regenerated raw materials often suffer from deterioration.[4,5] Chemical recycling has attracted increasing research interest in recent years.[4,6–9] Breaking the C–C, C–O, or C–N bonds in polymer backbones enables the transformation of post-consumer plastics into building blocks for new materials. For example, hydrogenolysis of polyolefins produces valuable products such as liquid fuels, waxes, and lubricants;[10–12] solvolysis of polyesters yields corresponding monomers or value-added derivatives;[4,13–16] and polyamides can be catalytically converted to either ε-caprolactam by a chain-end backbiting process or alcohols and amines by hydrogenolysis.[17,18] Despite the progress, the depolymerization of waste plastics often requires harsh conditions to achieve bond cleavage, undermining the economic viability of these processes. Therefore, developing cost-effective and energy-efficient chemical recycling processes plays a significant role in achieving a more sustainable future.

While chemical recycling is energy intensive, enzymatic depolymerization is performed under environmentally benign conditions. Several enzymes, such as hydrolase, peroxidase, and oxidase, have been demonstrated to have the ability to degrade polymers in the ambient environment. Enzymatic depolymerization of polyesters has been intensively investigated. Various types of hydrolases have been identified to degrade polyethylene terephthalate (PET), such as lipases,[19,20] cutinases,[21–23] and PETases.[24] Meanwhile, the protein engineering strategy has been employed to improve catalytic activity and thermostability of these PET-degrading enzymes. For instance, a disulfide bridge was introduced into leaf-branch compost cutinase (LCC) to improve its thermostability, and site-specific saturation mutagenesis was conducted to improve its specific activity.[25] Very recently, the highly labile PETase was engineered through a machine learning algorithm, resulting in a robust and active variant termed FAST-PETase.[26] FAST-PETase completely depolymerized many kinds of commercial post-consumer PET at 50 °C within one week. Polyolefins and polyamides are more challenging to depolymerize by enzymes compared with polyesters. Manganese peroxidase (MnP), lignin peroxidase, and laccase have been shown to cleave sp^3 C–C bonds in polyethylene (PE) at 37 °C,[27–29] although oxidation pretreatment or redox mediators are required in these processes.[30–32] In the case of low molecular weight PE, alkane hydroxylases from *Pseudomonas putida* can directly catalyze the depolymerization through the terminal oxidation mechanism.[33,34] Furthermore, a purified hydroquinone peroxidase has been demonstrated to accelerate the cleavage of C–C bonds in polystyrene (PS) in a dichloromethane–water system.[35] For polyamides, although various

State Key Laboratory of Chemical Engineering, Department of Chemical Engineering, Tsinghua University, Beijing 100084, China. E-mail: niuzq@tsinghua.edu.cn

† These authors contributed equally.

hydrolases (proteases, cutinases, and amidases) can facilitate their surface modification,[36–39] obvious mass loss and molecular weight decrease of polyamide can only be observed using MnP or a laccase-mediated system at 30 °C.[40] While these laboratory results suggest the feasibility of enzymatic plastic recycling, challenges related to the enzyme's activity, stability, and cost need to be further addressed. The main problem using enzymes is their poor stability upon temperature changes, pH fluctuations, and the presence of contaminants and additives in the plastic wastes. Furthermore, most enzymes can only catalyze the degradation of amorphous polymers.

The high efficiency of enzymatic plastic degradation inspires the development of biomimetic catalysts to reduce the energy consumption of plastic recycling. The field of synthetic enzymes is rapidly growing. Cyclodextrins,[29,41] crown ethers,[42] metalloporphyrins,[43] molecularly imprinted polymers[44,45] and other materials[46–48] have shown enzyme-like activities. These catalysts are generally more stable than natural enzymes and capable of functioning under a wide range of conditions. Designing enzyme-mimicking catalysts for plastic depolymerization has the potential to circumvent the need for harsh reaction conditions. So far, there are limited research studies on the mimicry of plastic-degrading enzymes. However, biomimetic catalysis applied to cellulose upgrading and deoxyribonucleic acid (DNA) hydrolysis is expected to promote the advancement of biomimetic plastic recycling due to the structural similarities.

In this perspective, we examine the current landscape of biomimetic catalysis for bond cleavage in plastics and related macromolecular substrates with specific focus on simulating both the active sites and the substrate-binding clefts of relevant enzymes. For the active sites, we discuss the mimicry of hydrolases for polyester hydrolysis, glycosidase for cellulose upgrading, peroxidase for plastic depolymerization and purple acid phosphatase mimetics for DNA hydrolysis. The role of the second coordination sphere is also discussed. In terms of substrate-binding clefts, emphasis is placed on molecular imprinting and diffusion control in porous materials to enhance the efficiency and selectivity toward polymer degradation. Through this discussion, we hope to elucidate the underlying principles and strategies for developing more efficient plastic-degrading catalysts.

2. Mimicking the active sites

The active site of an enzyme is a small part of the protein that directly binds to a substrate and promotes bond cleavage and formation. It is composed of several amino acid residues located in a three-dimensional cleft of the protein, sometimes including metal cations as co-factors.[49] The active site interacts with a substrate through non-covalent forces such as hydrogen bonding, π–π stacking, hydrophobic effects, electrostatic interactions, and van der Waals forces. These interactions are crucial for biocatalytic processes in terms of substrate confinement, organization and activation as well as transition state stabilization.[50,51]

Recent advances in protein isolation, purification, and characterization have uncovered the structure of the active sites in enzymes for macromolecule depolymerization.[52–55] This provides helpful information for chemists to mimic the structure or the function of these enzymes.[56] Organometallic complexes are frequently employed to mimic the functions of metalloenzymes.[57–61] In comparison, imitating the active sites composed solely of amino acids requires more efforts to accurately position the related functional groups in three dimensions. Previous studies have highlighted the catalyst design principles based on model substrates.[62,63] In this section, we will focus on the related work for plastic and cellulose depolymerization.

2.1. Hydrolase mimics for polyester depolymerization

Chemical depolymerization of PET needs high temperature (150–200 °C), increased pressure (20–40 atm), or concentrated acids and bases. Recent research has revealed that some microorganisms can break down PET under ambient conditions by producing hydrolytic enzymes such as cutinases,[21,22,25] lipases,[19,20] and PETases.[24] PETase has similar characteristics to lipases and cutinases such as having an α/β-hydrolase fold, but its active-site cleft is more open than those of cutinases. Fig. 1a shows the proposed mechanism for PET binding in this shallow cleft: when PET enters the groove, the ester carbonyl group is polarized by an anion hole and ready to be attacked by a nucleophilic hydroxyl group carried by a catalytic triad (serine, histidine, and aspartic acid).[55] The binding cleft confines the PET and nucleophile in close proximity to accelerate the hydrolysis rate.

Attempts have been made to directly replicate or modify the active site of PETase. Li *et al.*[64] combined PETase's catalytic triad with a self-assembling polypeptide (Fig. 1b). This enzyme mimic achieved a 16% weight reduction of a commercial PET film after a two-week incubation at pH 9 and 65 °C. However, the observed activity is not comparable to the performance of PETase. This implies that the amino acid residues can only exert optimal hydrolytic activity in a specific spatial conformation. Moreover, the application of this enzyme mimic is still constrained by limited thermostability and a narrow pH range. Hence, developing stable and highly efficient enzyme mimics by imitating the active site of PET hydrolase remains a challenge.

Instead of replicating the active site, imitating the mechanism of enzymatic depolymerization is also explored. As mentioned, an important reason why PET-degrading enzymes can achieve ester bond cleavage under ambient conditions is that the binding cleft can bring PET and nucleophile into proximity, thus increasing the effective concentration of the reactants. It is recognized that the proximity effect is also involved in other hydrolysis processes catalyzed by metallohydrolases, such as the organophosphate-degrading enzyme from *Agrobacterium radiobacter* (OpdA).[67] The active site of OpdA comprises two metal ions, one of which binds to the hydroxyl group while the other binds to the phosphate group (Fig. 1c), enabling facile nucleophilic attack. Synthetic analogs of OpdA are much easier to develop than those of PETase. Based on these considerations, a binuclear zinc complex (Zn_2L) was synthesized and exhibited catalytic activity for PET hydrolysis under

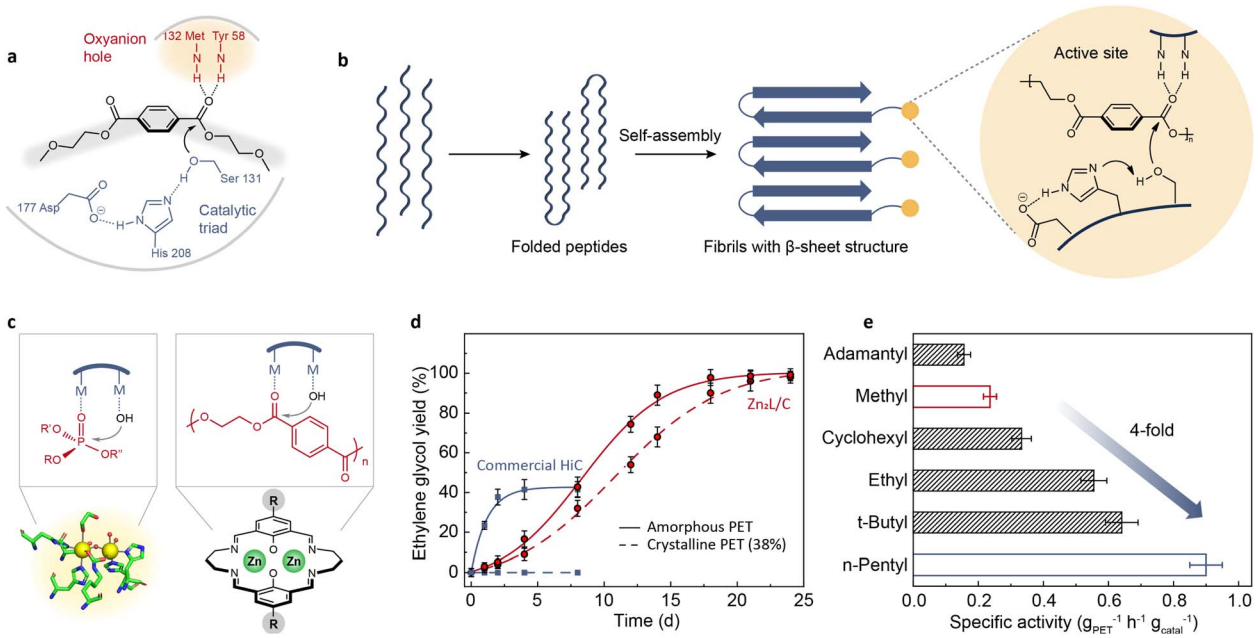

Fig. 1 (a) Schematic representation of the hydrolysis mechanism proposed for PETase.[55] Adapted with permission from ref. 55. Copyright 2017 Springer Nature. (b) PET hydrolase mimic obtained by self-assembly of polypeptide MAX.[64] Adapted with permission from ref. 64. Copyright 2023 Elsevier Inc. (c) Schematic diagram of the hydrolysis mechanism of OpdA and a hypothesized binuclear catalyst.[65] (d) Reaction kinetics of PET hydrolysis catalyzed by Zn_2L and commercial *Humicola insolens* cutinase (HiC) at pH 8 and 60 °C.[65] Adapted with permission from ref. 65. Copyright 2023 Springer Nature. (e) The specific activities of Zn_2L with different alkyl substituents for PET hydrolysis in a mixed solution of NaOH aqueous solution (0.1 M) and methanol (v/v = 4 : 1) at 60 °C.[66] Adapted with permission from ref. 66. Copyright 2023 The Royal Society of Chemistry.

a wide range of reaction conditions.[65] One advantage of Zn_2L was that its catalytic activity was not compromised too much for high-crystallinity PET, whereas the enzyme was completely inactive for the same substrate (Fig. 1d). Furthermore, Zn_2L was effective toward various post-consumer PET wastes and other types of polyesters. The catalytic activity of Zn_2L was further optimized by tuning the substituents in the *para* position of the macrocyclic ligand.[66] The electronic effects of the *para*-substituents can influence the binding strength of metal centers to the substrates. Hammett studies revealed a volcano-shaped correlation between the reaction rate and the Hammett constant. Guided by this structure–activity relationship, a more efficient catalyst (*n*-pentyl-substituted binuclear zinc complex) was identified, with a specific activity four times higher than that of the original methyl substitution (Fig. 1e). In addition to substituent modulation, changing the metal species in the metal complexes provides another way for enhancing activity, which has been verified in the literature.[65]

2.2. Glycosidase mimics for cellulose upcycling

Cellulose is a linear polysaccharide with glucose monosaccharide units connected by C–O–C linkages. Since C–O–C linkages are ubiquitous in many plastics (Fig. 2a), approaches for cellulose conversion could be used for plastic recycling. The upgrading of cellulose requires first depolymerizing it into soluble monomer sugars and oligosaccharides by breaking the stubborn glucoside bond, and then further transforming them into biofuels.[68] The enzymatic cleavage of glycosidic bonds in cellulose is typically facilitated by two carboxylate residues within the active sites of glycosidases.[69] The majority of glycosidases hydrolyze cellulose *via* either a double or single displacement mechanism, resulting in retention or inversion of the anomeric configuration, respectively.[69–71] The catalytic process *via* the double displacement mechanism involves one carboxylate amino acid residue serving as an acid/base and the other serving as a nucleophile (Fig. 2b). The single displacement mechanism entails typical acid–base catalysis, in which one amino acid residue activates water and the other protonates the glycosidic oxygen (Fig. 2c).[69–71]

As a pair of carboxylate residues is highly conserved in the active sites of most glycosidases,[69,72] the emulation of the active site of glycosidases was attempted by simply introducing carboxyl groups. For example, Shrotri *et al.* introduced carboxyl functional groups into activated carbon by oxidation (Fig. 2d).[73] They observed that increasing the oxidation temperature led to an increased density of carboxyl groups and thus the yield of hydrolysate (Fig. 2e). Similarly, acid–base pairs (*e.g.* COOH–COO^-, COOH–NH_2, and COOH-imidazole) have also been introduced into carbon materials or magnetic nanomaterials to mimic the active sites of glycosidase, aiming to obtain recyclable and stable biomimetic catalysts.[74–76] Although these catalysts can catalyze the cleavage of glycosidic bonds, their catalytic activity is far below that of the natural enzymes, because the acid–base pairs are randomly distributed on the material surface. The importance of spatial positioning of the acid–base pairs has been validated in cellobiose hydrolysis

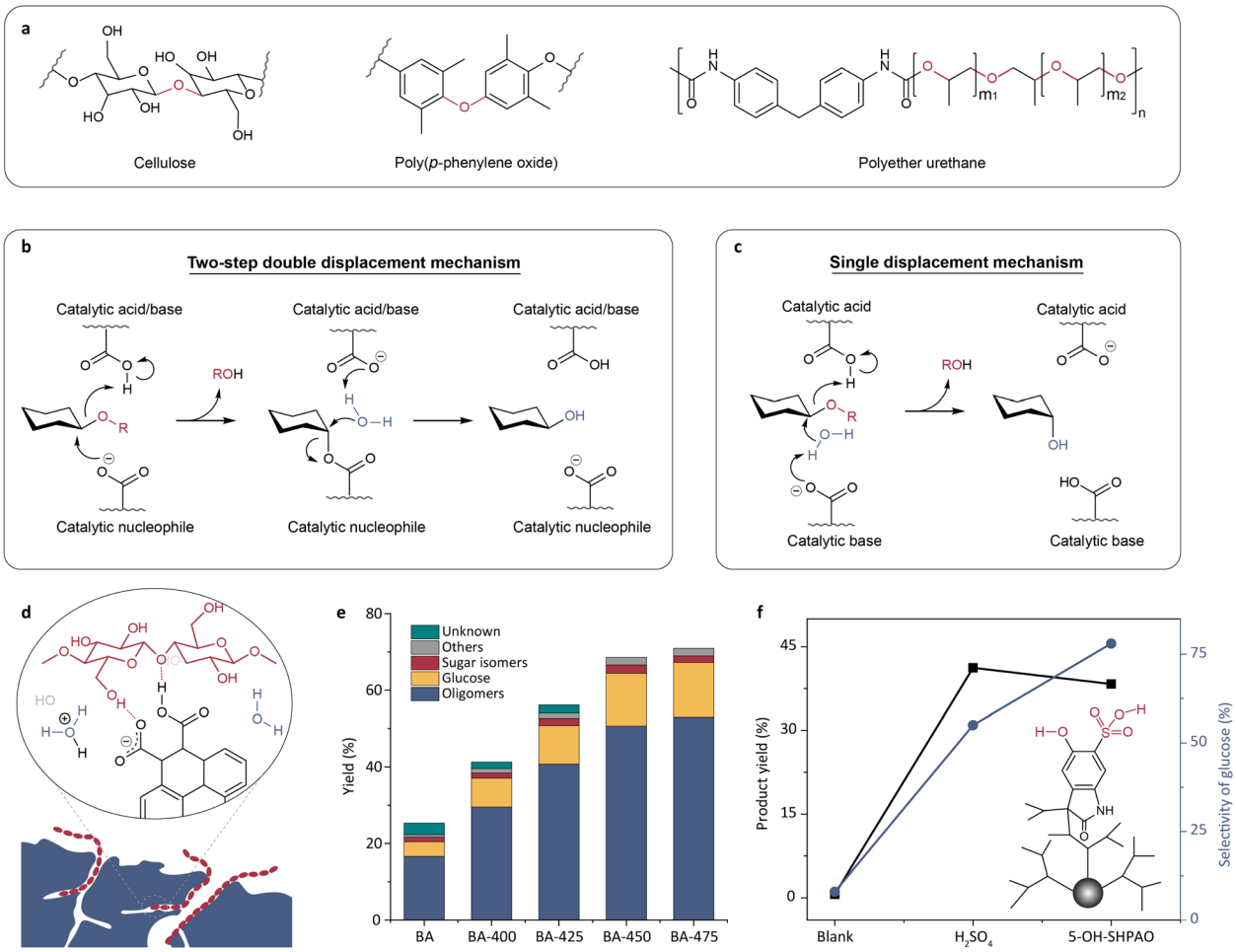

Fig. 2 (a) The structures of cellulose and plastics containing C–O–C linkages. (b and c) Schematic illustrations of the double displacement mechanism (b) and the single displacement mechanism (c) proposed for cellulose hydrolysis catalyzed by glycosidases.[71] Adapted with permission from ref. 71. Copyright 2022 Springer Nature. (d) A glycosidase mimic made by introducing carboxyl groups through oxidation of activated carbon.[73] (e) The effect of oxidation temperature on cellulose hydrolysis activity.[73] Adapted with permission from ref. 73. Copyright 2016 Wiley-VCH. (f) The comparison of cellulose hydrolysis with 5-OH-SHAPO, H_2SO_4, and without a catalyst.[78] Adapted with permission from ref. 78. Copyright 2016 The Royal Society of Chemistry.

catalyzed by organic acids.[77] The comparison of turnover frequency (TOF) values between *ortho*-, *meta*-, and *para*-hydroxybenzoic acids suggests that a vicinal acid–base pair significantly contributes to catalytic activity. High catalytic performance of adjacent acid–base pairs was also observed in the enzyme mimic designed by Yu *et al.*, using a sulfonated, hyperbranched poly(arylene oxindole).[78] The hydroxyl group and the neighboring sulfonic acid in the glycosidase mimic, 5-OH-SHAPO, synergistically catalyzed the depolymerization of cellulose. This enzyme mimic exhibited high catalytic activity and glucose selectivity comparable to those of inorganic acids (Fig. 2f). The above results suggest that developing enzyme mimics capable of reproducing the accurate spatial conformation of the active site will improve catalytic activity. Further discussion on this strategy will be presented in Section 3.

In addition to the precise positioning of acid–base pairs, researchers have developed another strategy to enhance the catalytic activity by introducing cellulose-binding domains in the catalyst design.[79] For example, a series of solid acid catalysts containing –Cl groups have shown enhanced cellulose hydrolysis rates compared to the corresponding catalysts without –Cl.[80–82] Similarly, the rate enhancement can also be achieved by introducing boronic acid groups ($-B(OH)_2$) into solid acid catalysts.[83] The functional groups (–Cl or $-B(OH)_2$) designed in these glycosidase mimics can bind cellulose by forming hydrogen bonds[80–82] or reversible covalent bonds[83] with the hydroxyl groups of cellulose, and thus improve mass transfer between the catalysts and cellulose and catalytic performance.

2.3. Peroxidase mimics for plastic depolymerization

As early as 1997, Deguchi and coworkers discovered that lignin-degrading fungi had the capability to degrade nylon.[84] Subsequently, MnP was identified from the fungi to be the enzyme that catalyzes nylon degradation.[85] After two days of incubation with MnP at 30 °C, a nylon film showed a 57% reduction in average molecular weight, and oxidative degradation

introduced new functional groups (–CH_3, –CHO, and –NHCHO). Peroxidase has also been reported to degrade acrylate polymers.[86–89] The hydroquinone peroxidase of the bacterium *Azotobacter beijerinckii* HM121 can rapidly degrade polyacrylamide and polyacrylic acid into small molecules in the presence of H_2O_2 and tetramethylhydroquinone at 30 °C.[87] Horseradish peroxidase was demonstrated to catalyze the radical degradation of partially hydrolyzed polyacrylamide.[88] Additionally, the crude peroxidase from *Trametes versicolor* CBR-04 has been reported to break down poly(potassium acrylate) at room temperature.[89]

Although research on mimicking peroxidase for plastic degradation remains limited to date, progress has been made for lignin depolymerization. Discussion in this field may provide valuable guidance for designing peroxidase mimics for plastic depolymerization or functionalization.

Peroxidases catalyze the oxidation of a substrate by peroxides such as H_2O_2. Most peroxidases contain the heme protein, with a central iron ion coordinated to a porphyrin ring.[90] Therefore, synthetic iron porphyrins are often used as models for heme peroxidases. The structure of synthetic iron porphyrins can be fine-tuned for enhanced activity and stability by adjusting axial ligands and substituents on the porphyrin ring, or even replacing an iron center with other metals. For instance, Zhu *et al.* synthesized a series of metallo-deuteroporphyrins as biomimetic catalysts for the oxidative conversion of lignin to aromatics (Fig. 3a–c).[91] By studying the catalytic activity on model substrates (2-(2-methoxyphenoxy)-1-phenylethanol), Co(DPDME) was identified as the best one in the M(DPDME) series (Fig. 3a). Furthermore, six Co-deuteroporphyrins with substituents of varying electron-donating capacities on the propionate side chains were designed to investigate the impact of these substituents on reaction activity and catalyst stability (Fig. 3b,c). Co(DPCys) was ultimately chosen as the catalyst for real lignin depolymerization owing to its capacity to catalyze the cleavage of C–O and C–C bonds in diverse lignin model compounds at room temperature (Fig. 3c). The liquid product yield from the real lignin depolymerization catalyzed by Co(DPCys) reached 31.2% after 10 hours at 150 °C, showcasing a 5.5-fold increase compared to the blank control.

In addition to regulating the central metal and the substituents of metalloporphyrin complexes, optimizing the microenvironment around the active site is another strategy to improve the catalytic performance. In natural peroxidases, the amino acid residues around the ferric center can help locate H_2O_2, facilitate the cleavage of the O–O bond, and stabilize the

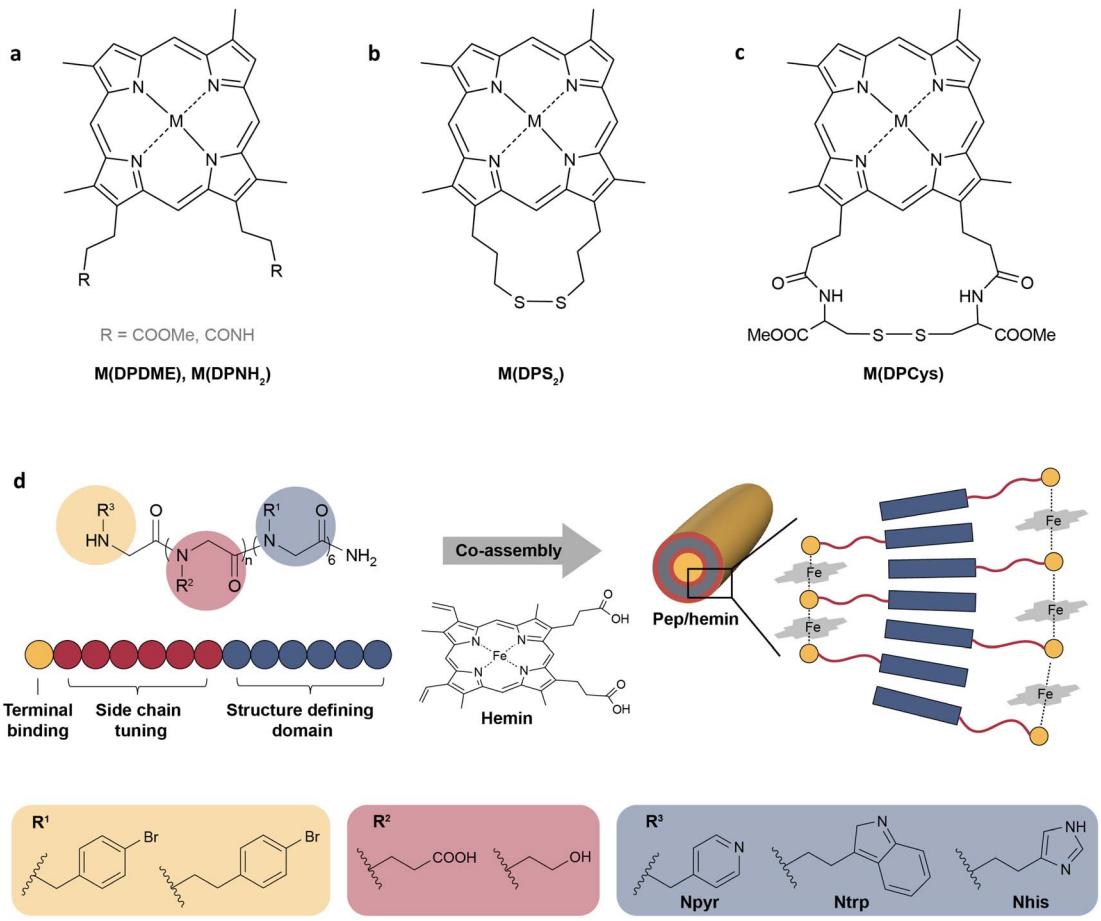

Fig. 3 (a–c) The structures of metallo-deuteroporphyrins designed for the catalytic depolymerization of lignin.[91] Adapted with permission from ref. 91. Copyright 2015 Wiley-VCH. (d) The schematic representation of self-assembled peptoid/hemin nanotubes.[92] Adapted with permission from ref. 92. Copyright 2022 Springer Nature.

high oxidation state of iron.[90] To imitate the function of the surrounding residues, a self-assembled peptide/hemin (Pep/hemin) nanomaterial was developed.[92] As shown in Fig. 3d, peptoid sequences with variations in the terminal binding site, polar side-chain domain length, and side chain group were synthesized, and then the peptoids were mixed and incubated with equimolar hemin to prepare Pep/hemin nanotubes (Fig. 3d). Among all the as-prepared nanotubes, Pep-1/hemin with the active site located at an optimal distance from the hydrophobic domain ($n = 6$), a carboxyl group on the side chain, and Npyr as terminal binding sites, showed the highest catalytic activity toward the oxidation of model compounds and surpassed all hemin-containing peroxidase mimics at the time. The self-assembled Pep/hemin not only enhanced catalytic activity but also demonstrated robustness at elevated temperatures in a wide pH range. Pep-1/hemin caused a 65.7% mass loss of lignin with a 61.7% yield of phenolic compounds after incubation at 60 °C for 2 h in the presence of H_2O_2. In addition to self-assembled peptides, the microenvironment has also been regulated by combining hemin-containing peroxidase mimics with metal–organic frameworks (MOFs),[93,94] graphene,[95] and supramolecular polymers.[96]

Various Fe-based, V-based and MOF-based materials have been reported to exhibit peroxidase-like activity,[93,97–100] providing additional references for developing peroxidase mimics for plastic depolymerization. Iron oxide nanoparticles are widely used in the biomedical field and environmental remediation due to their outstanding peroxidase-like activity.[99–101] This activity is attributed to the Fe^{2+}-induced Fenton and/or Haber–Weiss reactions.[97] In 2022, Liu and coworkers applied Fe_3O_4 nanoparticles for the removal and degradation of microplastics.[102] Fe_3O_4 nanoparticles can adsorb polypropylene (PP), PE, polyvinyl chloride, PS and PET microplastics from water through hydrogen bonding, and then they can be removed by magnetic separation. When heated at the melting temperatures of the respective plastics, almost 100% degradation of PP, PE, and PS was achieved by Fe_3O_4 in the presence of H_2O_2. The Fe_3O_4 nanoparticles can be easily recovered from the reaction solution and retained their original performance. Its stability and recyclability make it suitable for large-scale applications.

2.4. The second coordination sphere: lessons from phosphatase mimics

Metalloenzymes play crucial roles in essential life processes such as oxygen reduction and DNA hydrolysis. Although the metal ions and coordinating amino acids that make up metallohydrolases are limited, the functions of metallohydrolases vary greatly even with the same metal ions and ligands.[103,104] A typical example is that heme B serves as the active centers in various enzymes such as globulins, catalases, oxidases, oxygenases and so on.[90] What makes the difference is the second coordination sphere, which involves noncovalent interactions between ligands and substrates or ligands and ligands. Many reviews have detailed the roles played by the second coordination sphere in enzymatic reactions.[60,105] In general, the interactions within the second coordination sphere affect biocatalytic processes by orienting substrates, stabilizing transition states, changing the redox properties, and aiding product release.[60,106] Hence, many research groups are interested in designing synthetic complexes with a modified second coordination sphere to investigate their functions in activity and selectivity.

Here we use purple acid phosphatases (PAPs, E.C. 3.1.3.2) as an example to illustrate the importance of the second coordination sphere. PAPs are known for their ability to enzymatically hydrolyze a diverse range of phosphorylated compounds, a process heavily involving the participation of the second coordination sphere.[103] Mimicking PAPs has a theoretical basis and can promote the understanding of the function of the second shell in turn. PAPs are a kind of binuclear hydrolase characterized by heterovalent dual metal sites containing Fe(III) and M(II), where M can be Fe, Mn, or Zn. Taking kidney bean PAP for example, its active centers are composed of Fe(III) and Zn(II) sites which are bonded with oxygen and nitrogen atoms from tyrosine, aspartate, histidine residues and asparagine (Fig. 4a).[107] However, the majority of components within the first coordination sphere do not actively participate in the catalytic cycle as shown in Fig. 4. In contrast, the second coordination sphere including two protonated histidine residues assumes a pivotal role in accelerating the hydrolysis process. During the reaction (Fig. 4c), His202 and His295 bind to two oxygen atoms from phosphate ester by hydrogen bonding to stabilize the transition state, while His296 functions as a proton donor, facilitating the departure of the leaving group. Mutagenesis studies have validated the importance of histidine residues in the hydrolysis process.[108] In the following part, we will discuss the synthetic complexes as the mimics of PAPs and their role in accelerating the hydrolysis of DNA. Although the substrates are different, related work can provide a reference for the design of plastic hydrolysis catalysts.

Over the past few decades, considerable efforts have been dedicated to synthesizing analogs of PAPs. One research focus is to increase substrate affinity and direct the nucleophile to the phosphodiester linkages by introducing functional groups in the second coordination sphere. An *et al.* designed $[Cu(L1)_2(-Br)](ClO_4)_5 \cdot 6H_2O$ with quaternary ammonium-modified bipyridines as ligands to promote DNA hydrolysis.[109] The Br^- is easily replaced by OH^- in aqueous solution to form the active Cu–OH species (Fig. 5a). The distance between the hydroxyl and the quaternary ammonium ion is around 5.5–5.7 Å, similar to that of adjacent phosphodiesters in DNA (*ca.* 6 Å). Through electrostatic interactions, the quaternary ammonium binds to the neighboring phosphoryl oxygen atoms, allowing the DNA to be cleaved by the spatially adjacent nucleophile (OH or H_2O). Apart from a quaternary ammonium ion, easily protonated guanidyl groups can also electrostatically interact with phosphodiester groups. Tjioe *et al.* introduced protonated guanidyl groups to copper(II) complexes with 1,4,7-triazacyclononane ligands.[110] Compared with non-guanidinylated analogs, a 22-fold enhancement in the hydrolysis rate has been achieved. This is because protonated guanidyl attracts the phosphodiester linkage and orients the nucleophilic Cu–OH to the phosphodiester group.

Another research endeavor is focused on stabilizing the transition state by using the second coordination sphere. Since

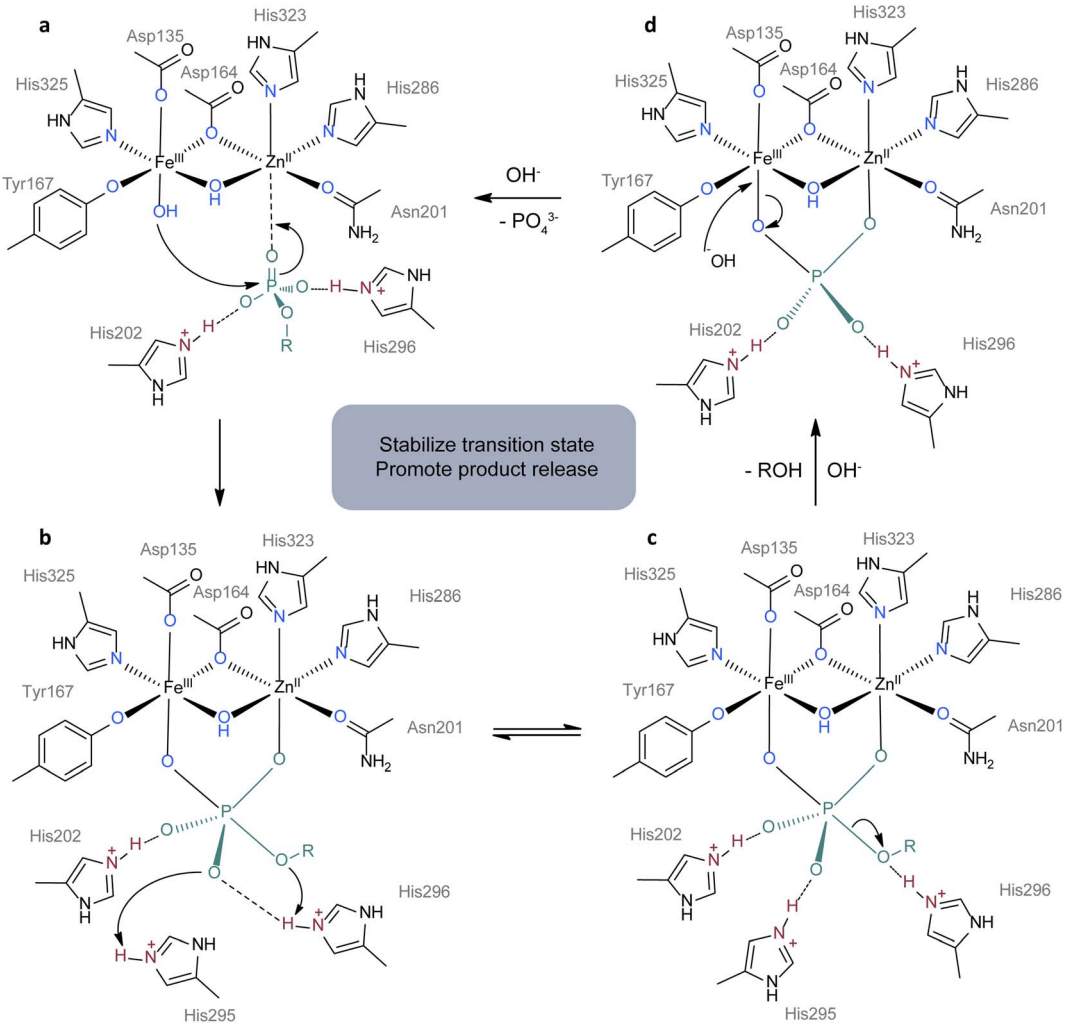

Fig. 4 Proposed mechanism for the hydrolysis of phosphomonoesters by kidney bean purple acid phosphatase.[107] (a) The substance is oriented for attackment of Fe^{III}–OH by interactions with Zn^{II}, His202 and His296. (b) RO group in subtance attacks protonated His296 and O atom attacks protonated His295. (c) P–O bond breaks with the release of ROH. (d) A hydroxide ion attacks Fe^{III} with the release of the phosphate group to start another cycle of catalysis. The first coordination sphere, second coordination sphere and substrate are colored in blue, red and green. Adapted with permission from ref. 107. Copyright 1996 Academic Press.

DNA is negatively charged in aqueous solution, positively charged groups in the catalyst can electrostatically attract substrates and accelerate the release of products. Aliphatic amines are of particular interest due to their ability as hydrogen donors and their electrostatic interactions with the phosphodiester backbone of DNA. As shown in Fig. 5b, the first coordination sphere of PAPs is extensively mimicked by an asymmetric chelating ligand H_2L^1, whereas the second coordination sphere can be reproduced by chemical modification with aliphatic amines. Based on this ligand, de Souza *et al.* synthesized a PAP analogue and covalently grafted it onto polyethyleneimine (PEI) to mimic the histidine residues in the polypeptide chain (Fig. 5c).[111] The as-obtained catalyst was termed FeCuL1-PEI. During DNA hydrolysis, the terminal amino groups of FeCuL1-PEI were protonated, facilitating the electrostatic interactions between the catalyst and DNA substrate. Moreover, the activation energy for DNA hydrolysis was lower on FeCuL1-PEI than on FeCuL1, which can be attributed to the stabilization of the negatively charged transition state and the formation of hydrogen bonds. A k_{cat}/K_M value of 2.7×10^4 h^{-1} M^{-1} for FeCuL1-PEI was record high among PAP molecular models at the time. In another example, Silva *et al.* introduced ethylene diamine and butene diamine to a H_2L^2 ligand and synthesized H_2L^2-et and H_2L^2-but (Fig. 5b), respectively.[112] They employed these two modified ligands to construct $Fe^{III}Zn^{II}$-based PAP analogues and studied the influence of the length of diamine on their hydrolysis activity. Compared with $Fe^{III}Zn^{II}L^2$ (without diamines), the diamine group enhanced the k_{cat}/K_M by 134% and 114% for $Fe^{III}Zn^{II}L^2$-et and $Fe^{III}Zn^{II}L^2$-but, respectively. According to the calculated energy minima, the terminal amino group of $Fe^{III}Zn^{II}L^2$-et was spatially closer to DNA than $Fe^{III}Zn^{II}L^2$-but's, leading to more stable interaction between DNA and the complex.[112]

Studies on PAP mimics can help develop antibiotics and antitumor drugs for the cleavage of target DNA. Camargo *et al.* synthesized $Fe^{III}Zn^{II}$LP1 and $Fe^{III}Zn^{II}$LP2 by introducing a pyrene

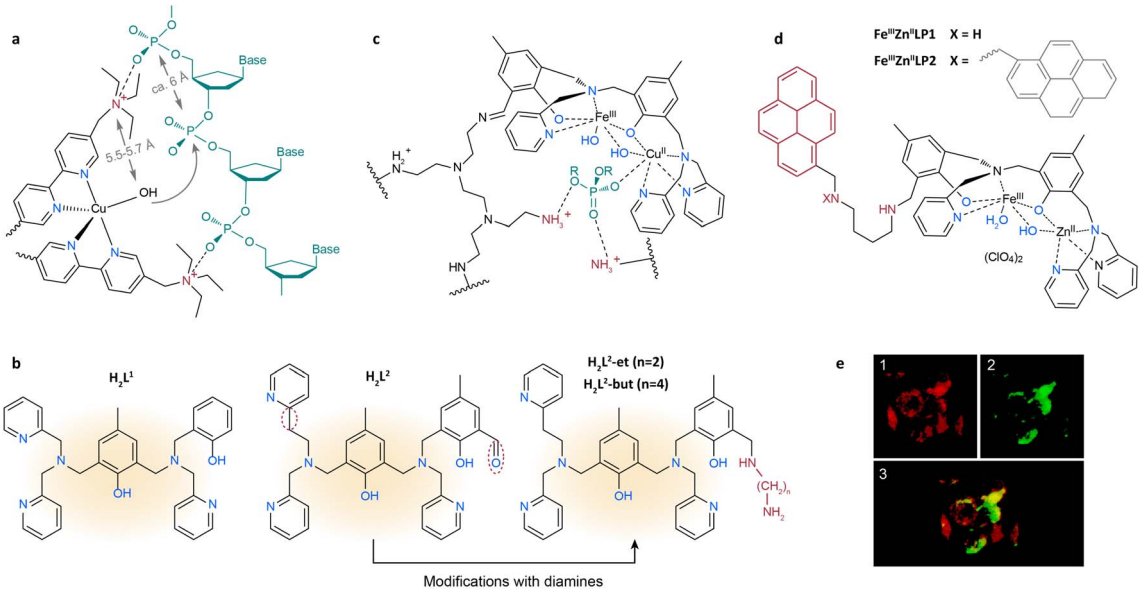

Fig. 5 (a) The proposed intermediate of DNA cleavage by $[Cu(L1)_2(Br)](ClO_4)_5 \cdot 6H_2O$, where L1 is 5,5′-di(1-(triethylammonio)methyl)-2,2′-dipyridyl.[109] Adapted with permission from ref. 109. Copyright 2006 The Royal Society of Chemistry. (b) The structures of H_2L^1, H_2L^2, H_2L^2-et and H_2L^2-but.[112] Adapted with permission from ref. 112. Copyright 2017 The Royal Society of Chemistry. (c) The proposed structure for the FeCuL1-PEI system with a bound phosphate diester.[111] Adapted with permission from ref. 111. Copyright 2013 American Chemical Society. (d) The structures of $Fe^{III}Zn^{II}$LP1 and $Fe^{III}Zn^{II}$LP2.[113] (e) Accumulation of $Fe^{III}Zn^{II}$LP1 in lysosomes, where $Fe^{III}Zn^{II}$P1 is pseudocolored in green (1) and the lysotracker in red (2).[113] Adapted with permission from ref. 113. Copyright 2017 American Chemical Society. The substrate and first and second coordination spheres are colored in green, blue and red, respectively, unless specified.

group to the H_2L^1 ligand (Fig. 5d) to enhance the affinity between DNA and the catalysts.[113] Due to the π–π stacking interaction in the second coordination sphere, all of the supercoiled plasmid DNA was converted to the open circular and linear forms at pH 7.0 in the presence of $Fe^{III}Zn^{II}$LP2 after 16 hours. The apoptosis ratio of K562 cells (from a human chronic myelogenous leukemia cell line) treated with $Fe^{III}Zn^{II}$LP1 was six times higher than the apoptosis ratio of those treated with $Fe^{III}Zn^{II}$L1. The colocalization of $Fe^{III}Zn^{II}$LP1 with lysosomes further indicated its potential as a novel antitumor drug (Fig. 5e).[114]

Asides from PAP mimics, tuning the second coordination sphere of natural enzymes has also been demonstrated to accelerate various reactions, such as CO_2 reduction, hydrogen evolution, hydrolysis of glycosidic bonds and so on.[115–117] Although the second coordination sphere effects have hardly been studied in the field of plastic depolymerization, many kinds of groups in polymer substrates can be involved in non-covalent interactions. For example, the aromatic groups in PS and PET can potentially participate in π–π stacking. The ester groups in polyesters and the amide groups in polyamides such as nylon-6 can be regarded as hydrogen bond acceptors and donors. We envision that mimicking the second coordination sphere through ligand design may be a new opportunity to achieve catalytic depolymerization of plastics under mild conditions.

3. Mimicking the substrate-binding cleft

Substrate-binding clefts significantly influence substrate specificity and reaction selectivity in enzyme catalysis. For instance, adenosine triphosphate (ATP)-dependent proteases feature protease domains with a unique six-fold symmetry (Fig. 6a).[118] This symmetry is altered by ATP to switch between "open" and "closed" interdomain contacts. These ATP-regulated orientations effectively restrict the access of a substrate to catalytic sites in a specialized tunnel. Cellobiohydrolase follows a similar mechanism for cellulose degradation.[119,120] It possesses a long tunnel where cellobioside binding occurs. As the cellulose chain threads further into this tunnel, it undergoes catalytic transformation. Interactions between the substrate and enzymes' cleft have also been identified in the enzymatic degradation of plastics. Mechanistic studies of PETase demonstrated that PET chains are guided to the vicinity of the catalytic triad through a π–π stacking between the PET benzene ring and the tryptophan residues in the shallow cleft (Fig. 6b).[121] This action allows for the selective, processive depolymerization of the polymer. These insights into substrate-binding clefts offer catalyst design principles for the degradation of targeted substrates ranging from biological macromolecules to plastic wastes.

3.1. Creating clefts *via* molecular imprinting

Molecularly imprinted polymers (MIPs) have been developed to emulate substrate-binding clefts. The imprinting strategy allows for a desired cavity that has multiple interactions with a specific template molecule in the polymer matrix.[122] Zhao and coworkers synthesized a variety of glycosidase mimics with cellulose hydrolysis activity using molecularly imprinted polymers.[72,123] As shown in Fig. 6c, a mixed micelle containing template molecules, free radical cross-linkers, and photo initiators was initially formed. Subsequently, the template

molecules were removed, resulting in a cleft, which was then post-modified to attain the desired geometrically and chemically fitting structure. Designing enzyme mimics *via* this strategy not only introduces the active site, but also tailors the size and depth of the cleft in the matrix by changing the template molecules. Nevertheless, molecularly imprinted enzyme mimics were less active than natural enzymes.[123] This gap could be attributed to several limitations of imprinted polymers, such as structural rigidity, inhomogeneity in binding sites, and limited mass transfer within the system.[44,122] These limitations particularly affect the catalytic activity when the substrates are macromolecules like plastics. Promising strategies have emerged to address these issues, such as downsizing MIPs using microgels,[122] integrating porous materials to produce highly cross-linked MIPs,[124,125] incorporating highly active nanozymes[126] and so on. These advances hold great promise for the application of the molecular imprinting approach in plastic degradation.

3.2. Mimicking clefts using porous materials

In the context of polyolefin depolymerization, the emulation of a substrate-binding cleft has been focused on tuning the interactions between polymer chains and porous materials. The interfacial interactions are initially investigated between porous filters and polymers in early research.[127,128] Duan *et al.* offered

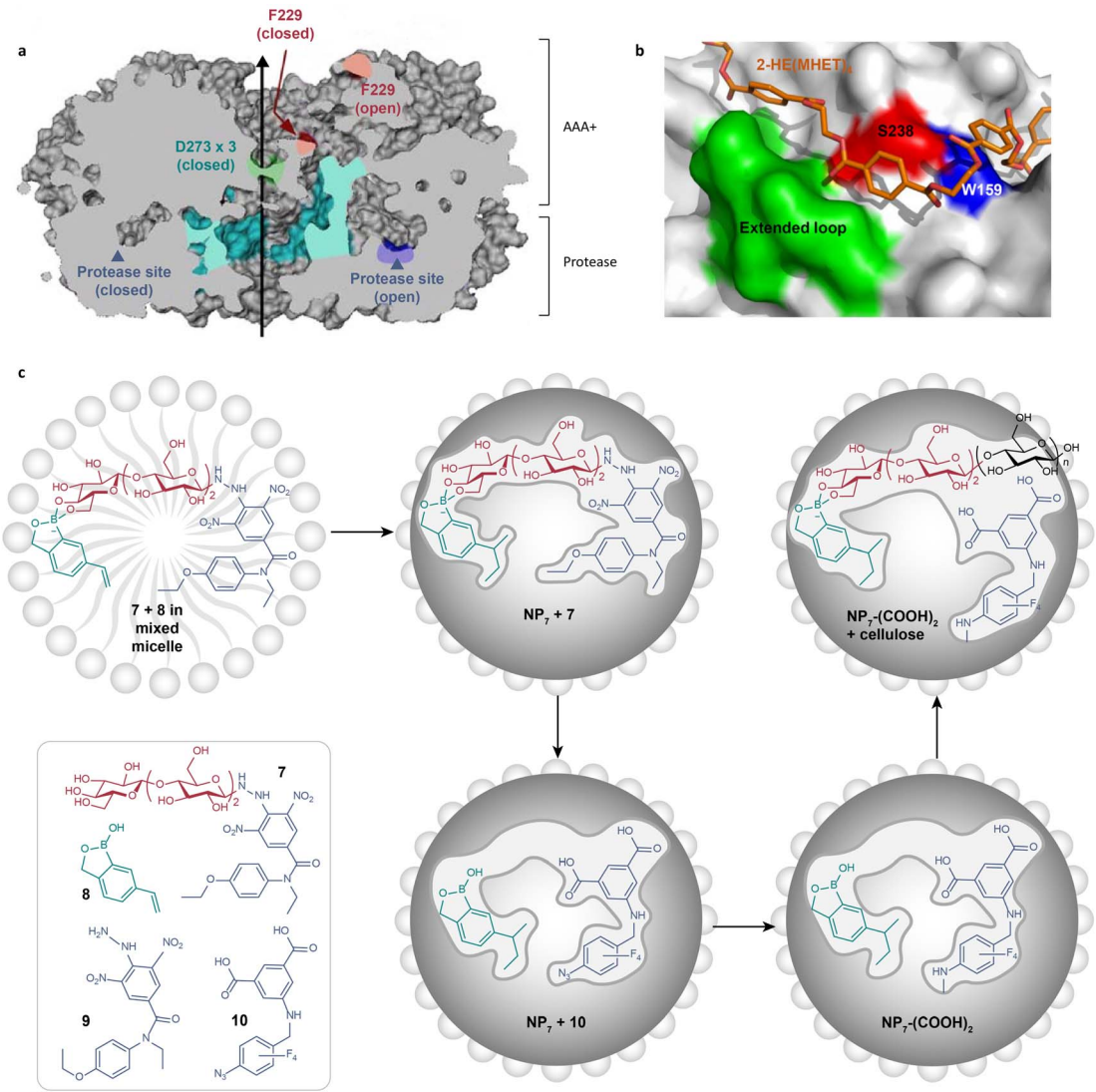

Fig. 6 (a) A diagram showing a cross-section of triple-symmetric FtsH, including the three-fold axis (depicted by a black line) and two protease active sites (indicated by Aegean blue arrowheads). AAA+ means ATPases associated with various cellular activities.[118] Adapted with permission from ref. 118. Copyright 2006 Elsevier Inc. (b) The structure of subsite II of *I. sakaiensis* PETase (*Is*PETase).[121] The structure of *Is*PETase is presented as surface models in gray color. The 2-hydroxyethyl-(monohydroxyethyl terephthalate)$_4$ docking model is shown in orange color. The residues S328 and W159, as well as the extended loop of *Is*PETase, are specifically labeled, which are crucial for forming the shallow and continuous clefts in subsite II and high hydrolytic activity of *Is*PETase. Adapted with permission from ref. 121. Copyright 2018 Springer Nature. (c) The preparation route of exocellulase mimics (NP$_7$–(COOH)$_2$) through the molecular imprinting approach.[72] Adapted with permission from ref. 72. Copyright 2022 American Chemical Society.

insights into this behavior by comparing the infiltrations of poly(vinylidene fluoride) (PVDF) and poly(ethylene oxide) (PEO) into porous UiO-66.[129] As shown in Fig. 7a, PEO fully infiltrated into the pores of UiO-66 due to stronger site-to-site interaction with O-(PEO) and the terminal OH groups on the Zr nodes of UiO-66. In contrast, PVDF exhibited limited infiltration into UiO-66 because of the weaker interaction between F-(PVDF) and the terminal OH groups.

The studies of the interfacial interactions between the inorganic porous phase and continuous polymeric phase have

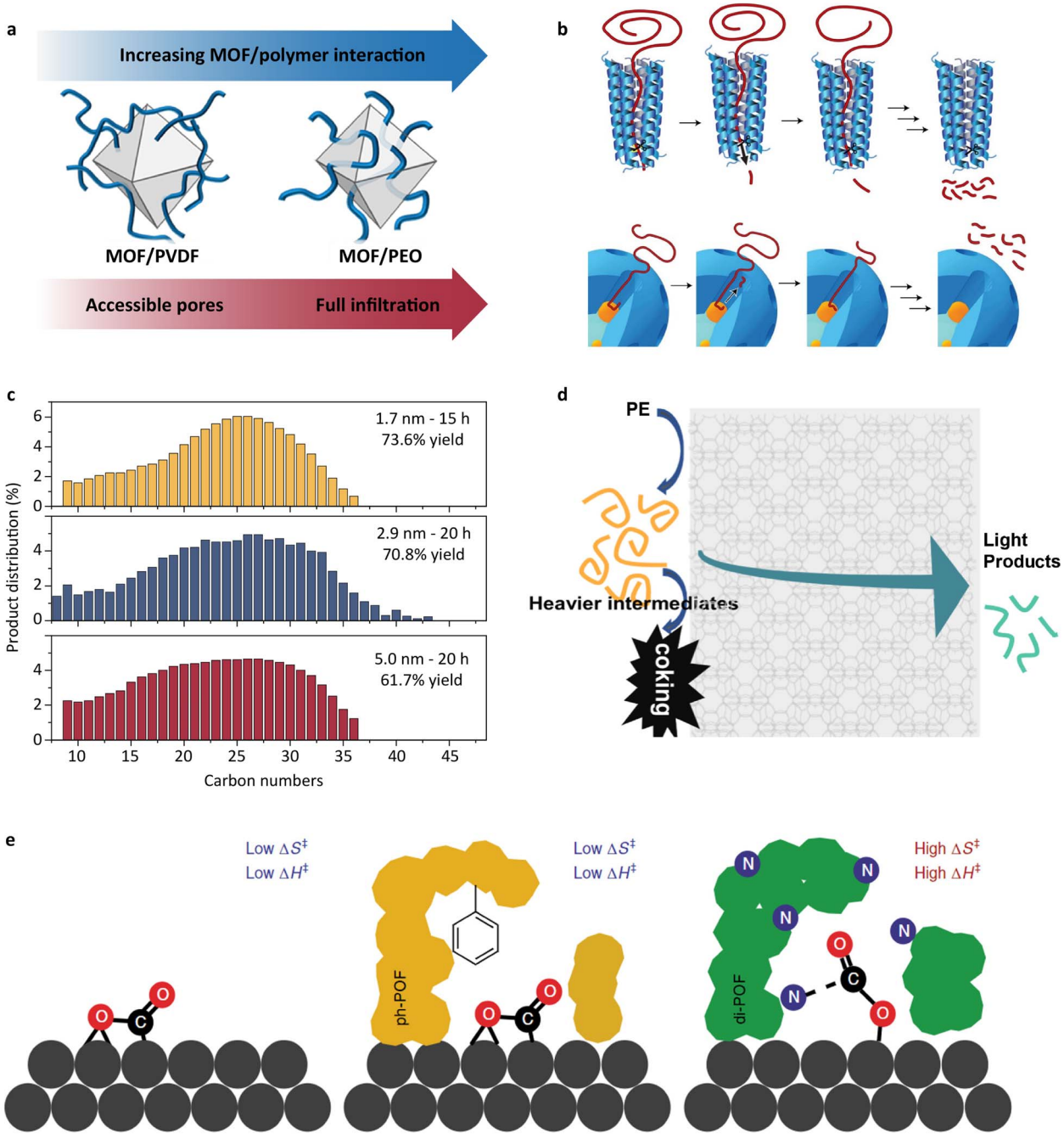

Fig. 7 (a) Schematic illustration of the infiltration of PVDF and PEO into UiO-66.[129] Adapted with permission from ref. 129. Copyright 2019 American Chemical Society. (b) The processive mechanism through which many enzymes deconstruct large macromolecules and an analogous mechanism proposed for the $mSiO_2/Pt/SiO_2$ catalyst.[11] Adapted with permission from ref. 11. Copyright 2020 Springer Nature. (c) Carbon number distributions of wax products from polyethylene hydrogenolysis using $mSiO_2/Pt\text{-}x/SiO_2$ (x: the mean Pt nanoparticle diameter). Top: $mSiO_2/Pt\text{-}1.7/SiO_2$; center: $mSiO_2/Pt\text{-}2.9/SiO_2$; bottom: $mSiO_2/Pt\text{-}5.0/SiO_2$.[130] Adapted with permission from ref. 130. Copyright 2022 American Chemical Society. (d) Schematic illustration of the cascade cracking steps on the external zeolite surface and within zeolite micropores on n-ZSM-5.[131] Adapted with permission from ref. 131. Copyright 2022 American Chemical Society. (e) The proposed transition state models for exposed Pd surfaces (such as in Pd/Al_2O_3 and Pd/POF), non-interacting POF-covered Pd surfaces (such as in ph-POF/Pd/POF) and strongly interacting POF layers (such as in POF/Pd/POF and di-POF/Pd/POF), respectively.[132] Adapted with permission from ref. 132. Copyright 2019 Springer Nature.

inspired researchers to introduce the concept of a substrate-binding cleft into the catalyst design for plastic depolymerization. Perras and coworkers designed a core–shell material for the degradation of waste polyolefins.[11] This core–shell catalyst consists of Pt nanoparticles supported on SiO_2 as the core and porous SiO_2 as the shell. Through solid-state nuclear magnetic resonance analysis, they confirmed that polyethylene chains diffused into the pores of the SiO_2 shell and interacted with the active sites in the core. Importantly, the diffusion rate of the polymer chains could be controlled by tuning the pore size, thereby influencing the product distribution. They likened this to an enzyme-like progressive depolymerization mechanism and correlated the selectivity with a "headfirst" adsorption of the polymer chains (Fig. 7b). In specific, the polymer chains adopt a straightened conformation navigating the narrow pores of the shell to reach the active sites situated at the core. The cleavage of the C–C bonds occurs at regular intervals, a process regulated by the diffusion rate of the polymer chains. Further research on the core–shell structure was conducted by Wu *et al.*,[130] focusing on how changes in the activity affect this progressive mechanism. It was found that the rate of C–C bond cleavage can be modulated by changing the size of Pt nanoparticles, while the product distribution remained nearly constant (Fig. 7c). This phenomenon suggests that the progressive mechanism is independent of the activity of the core–shell catalysts. Another research study on an "open–open" pore structure was recently reported by Tennakoon *et al.*[133] This structure facilitated a faster diffusion rate of the products from the active sites compared with the traditional "open-end" core–shell structure. This diffusion behavior can avoid over-hydrogenolysis and thus achieves a very low yield of volatile products. These results highlight that the structure designed substrate-binding clefts tuned the selectivity *via* controlling the polymer chains' diffusion rate in its designed structure.

Designing porous materials to mimic substrate-binding clefts can also alter selectivity by influencing reaction mechanisms. Zhao *et al.* found that the product distribution of PP pyrolysis narrowed from the C_3–C_{15} range in the blank group to C_4–C_9 in the presence of HY zeolites.[134] Meanwhile, cyclic hydrocarbons were detected in the presence of HY, whereas they were absent in the blank group. This suggests that PP pyrolysis follows not only the free radical mechanism but also the ionic mechanism. The effect of pore size on the product distribution was also observed in the catalytic pyrolysis of mixed PP and PE.[135] ZSM-5 showed higher selectivity for olefins than USY, while USY generated more paraffins and coke than ZSM-5. This difference may result from hindrance of bimolecular reactions in the 10-membered-ring channels of ZSM-5, whereas the 12-membered-ring pores of USY allowed for these reactions to occur. This implies that the diffusion limitation of intermediate products in zeolites can change the product distribution by influencing reaction types. Catalytic pyrolysis of model

Table 1 Summary of biomimetic catalysts for the depolymerization of macromolecules

	Enzyme mimics	Conversion (%)	Conditions	Ref.
PET hydrolysis	Self-assembled peptide	16[a]	pH 9, 65 °C, 2 weeks	64
	Binuclear zinc complex	100	pH 8, 40 °C, 10 weeks	65
	n-Pentyl-substituted binuclear zinc complex	100	80% 0.1 M NaOH solution + 20% CH_3OH, 60 °C, 10 h	66
Cellulose hydrolysis	COOH-functionalized carbon	96	180 °C, 20 min	73
	5-OH-SHAPO	62	150 °C, 5 h	78
	Solid acid containing –Cl and $-SO_3H$	46[b]	180 °C, 12 h	80
	Porous polymers bearing boronic and sulfonic acids	94.6[c]	120 °C, 48 h	83
	Molecularly imprinted synthetic glucosidase	15.8[d]	pH 5, 90 °C, 12 h	123
	A blend of cellulase-mimicking polymeric nanoparticles	40.4[d]	pH 6.5, 90 °C, 12 h	72
Lignin oxidation	Co(DPCys)	31.2	150 °C, 10 h, oxone	91
	Pep-1/hemin	61.7[e]	60 °C, 3 h, H_2O_2	92
Microplastic degradation	Fe_3O_4 nanoaggregates	100 for PE and PS, 95 for PP, 64 for PET[a]	12 h, H_2O_2, 150 °C for PE, 200 °C for PS, 140 °C for PP, 240 °C for PET	102
DNA hydrolysis	$[Cu(L1)_2(Br)](ClO_4)_5$	100	pH 7.2, 37 °C, 1 h	109
	FeCuL1-PEI	45[f]	pH 7.0, 37 °C, 24 h	111
	$FeZnL^2$-et	63[f]	pH 7.0, 50 °C, 4 h	112
	FeZnLP1	95	pH 7.0, 37 °C, 16 h	113
	FeZnLP2	100		
PE hydrogenolysis	$mSiO_2/Pt/SiO_2$	6.7[g]	1.38 MPa H_2, 250 °C, 6 h	11
	$mSiO_2/Pt/MCM$-48	35.4[g]	2.06 MPa H_2, 300 °C, 6 h	133

[a] Weight loss. [b] Yield of levulinic acid. [c] Yield of glucose. [d] Yield of reducing sugar. [e] Yield of phenolic compounds. [f] Product: open circular DNA. [g] High density PE as the reactant.

compounds clearly demonstrated this effect.[136] Small pore size (<6.1 Å) zeolites mainly promoted the cleavage of long-chain hydrocarbons with little benzene, toluene, and xylene (BTX) produced, because the pore size is insufficient for these aromatic products to diffuse. Large pore size (≥6.1 Å) zeolites can further catalyze aromatization and hydrogen transfer reactions to produce BTX and paraffins. By mimicking the substrate-binding cleft using porous materials, the diffusion and reaction of polymers and intermediates can be tuned, thereby altering the product distribution.

3.3. The challenge in selectivity control

The role of substrate-binding clefts in affecting reaction activity and selectivity is crucial. However, the efficiency of this strategy lies in the precise positioning of the active sites. Often times, a polymer chain can navigate and react within a pore, but the desired selectivity cannot be achieved in the absence of accurate positioning. Polyethylene hydrocracking catalyzed by zeolites evidences this point (Fig. 7d). The Brønsted acid sites in zeolites act as the primary active centers for cracking. When Brønsted acid sites are uniformly distributed across the zeolite structure, the product distribution for polyethylene cracking appears similar among different zeolites, predominantly falling within the C_2 to C_9 range.[131,137,138] Future studies need to give more considerations to the appropriate positions of the active sites in the porous matrix to regulate the product distribution.

While it has been shown that the diffusion of polymers in porous materials is pore-size-dependent, the chemical feature of the functional groups on the inner surface of the pores can be another important factor.[129,139] Riscoe *et al.* offered an approach into this dimension (Fig. 7e). They crafted a polymer–nanocrystal hybrid to tailor CO_2 diffusion by modulating the functional groups inside the pores including the phenyl and the amino groups.[132] It turned out that the amino group has lower adsorption enthalpy toward the CO_2 product, because N atoms interact with the CO_2 product and reduce its diffusion rate in the pores. The strategy of surface functionalization could be more widely used in catalyst design in the future. For instance, adding hydrophilic functional groups into the SiO_2 pores might reduce the PE diffusion rate thus altering the selectivity. In addition, tuning the density and chemical feature of the functional groups is more precise than controlling the pore size. It is expected that more efforts will be dedicated to this area.

4. Conclusions and perspectives

The urgency of plastic pollution has stimulated extensive research into chemical recycling processes and plastic-degrading enzymes. Biomimetic catalysis has been demonstrated to be effective in degrading macromolecules under mild conditions (Table 1). This perspective has underscored two main approaches to mimic the plastic-degrading enzymes: imitating the active sites and the substrate-binding cleft. The active sites play a key role in activating and transforming substrates. Directly replicating the active site of plastic-degrading enzymes is highly challenging because their active sites are composed of a network of amino acid residues with intricate positioning. Alternatively, the structural emulation of binuclear esterases has been well-developed by following similar catalytic mechanisms. These esterases contain two metal centers and utilize the proximity effect to enhance the effective concentration of substrates locally during hydrolysis. The mimicry of the active centers of binuclear esterase has shown excellent polyester hydrolysis activity even under weakly alkaline or near-neutral conditions.[140] In addition to metallic centers, the second coordination sphere often plays subtle yet crucial roles in stabilizing key intermediates through non-covalent interactions. Therefore, it is anticipated that the regulation of the functional groups in the second coordination sphere, for instance by introducing auxiliary ligands in metal complexes, would further improve the catalytic activity of enzyme mimics thus facilitating plastic depolymerization under mild conditions.

On the other hand, enzymes typically feature a substrate-binding cleft ensuring the specificity for the substrate and the selectivity of the product. This structure facilitates enzymes to degrade polymers in a processive manner in some cases. The molecular imprinting approach has been employed to emulate the enzyme's cleft, proving effective in cellulose hydrolysis. Nevertheless, this technique encounters limitations when applied to plastics. Porous materials have been introduced to mimic the interaction between the substrate and clefts in the enzyme, as demonstrated in core–shell materials, molecular sieves, and metal organic frameworks. These porous materials exhibit good stability, ease of synthesis, and mouldability of sites compared to molecule enzyme mimics. It has been verified that the product distribution of PE depolymerization is significantly affected by the pore size of the catalyst. It should be noted that the substrate-binding cleft in these biomimetic catalysts lacks the flexibility observed in natural enzymes, which is crucial for adjusting the active site and accommodating substrates.

From the above discussion, we can distill all these studies down to the following design principles:

(1) Active site: The essence of mimicking active sites is not just in replicating their exact structural nuances but also in emulating their reaction pathways. A profound understanding of the enzymatic reaction mechanism is paramount and should be the cornerstone of the catalyst design.

(2) Cleft: Porous materials are often employed to mimic the function of enzyme clefts. Adjusting pore sizes has proven effective in modulating polymer chain diffusion rates and enhancing selectivity to some extent. Altering the functional groups within the pores could be promising to achieve improved diffusion control of polymeric substrates.

(3) Synergy: The collaboration between the active site and the substrate-binding cleft is more important than imitating the function of the two alone. However, this synergy relies on the precise positioning of both the active site and the cleft. Their orchestrated alignment might unlock unprecedented catalytic efficiencies. Although the molecular imprinting strategy has shown great potential in simulating synergistic interactions during catalytic conversion of cellulose and small molecules,

polymer depolymerization may require the integration of other approaches to address constrained mass transfer and poor stability issues. Developing biomimetic catalysts with a flexible cleft near active sites may potentially contribute to addressing constrained mass transfer issues. This may be achieved by incorporating materials such as peptides and peptoids into biomimetic catalysts.

Applying the aforementioned design principles, scientists have demonstrated the significance of biomimetic catalysis in recycling polyester and polyolefin plastics. A persistent challenge still lies in tailoring enzyme mimics to achieve substrate specificity, product selectivity, and high activity for plastic depolymerization, which are crucial for addressing complex real-world solid wastes. The application of biomimetic catalysis in plastic recycling is steadily gaining momentum, and we hope that this perspective will help bridge the gap between chemical recycling of plastics and enzyme-catalyzed macromolecular depolymerization.

Author contributions

Z. N. conceived the perspective and edited the manuscript. Y. W., Q. H., and Y. C. conducted literature review and prepared the first draft of the manuscript. The manuscript was written through contributions of all authors.

Conflicts of interest

The authors declare no conflict of interest.

Acknowledgements

This work was supported by the National Natural Science Foundation of China (22375113 and 22075162), the National Key R&D Program of China (2019YFA0709200), the Tsinghua University Initiative Scientific Research Program (20221080067), and Ordos Laboratory (Ordoslab-2024014).

References

1 J. R. Jambeck, R. Geyer, C. Wilcox, T. R. Siegler, M. Perryman, A. Andrady, R. Narayan and K. L. Law, Plastic waste inputs from land into the ocean, *Science*, 2015, **347**, 768–771.

2 M. MacLeod, H. P. H. Arp, M. B. Tekman and A. Jahnke, The global threat from plastic pollution, *Science*, 2021, **373**, 61–65.

3 A. Chamas, H. Moon, J. Zheng, Y. Qiu, T. Tabassum, J. H. Jang, M. Abu-Omar, S. L. Scott and S. Suh, Degradation Rates of Plastics in the Environment, *ACS Sustainable Chem. Eng.*, 2020, **8**, 3494–3511.

4 C. Jehanno, J. W. Alty, M. Roosen, S. De Meester, A. P. Dove, E. Y. Chen, F. A. Leibfarth and H. Sardon, Critical advances and future opportunities in upcycling commodity polymers, *Nature*, 2022, **603**, 803–814.

5 I. Vollmer, M. J. F. Jenks, M. C. P. Roelands, R. J. White, T. van Harmelen, P. de Wild, G. P. van der Laan, F. Meirer, J. T. F. Keurentjes and B. M. Weckhuysen, Beyond Mechanical Recycling: Giving New Life to Plastic Waste, *Angew. Chem., Int. Ed.*, 2020, **59**, 15402–15423.

6 A. J. Martín, C. Mondelli, S. D. Jaydev and J. Pérez-Ramírez, Catalytic processing of plastic waste on the rise, *Chem*, 2021, **7**, 1487–1533.

7 G. W. Coates and Y. D. Y. L. Getzler, Chemical recycling to monomer for an ideal, circular polymer economy, *Nat. Rev. Mater.*, 2020, **5**, 501–516.

8 F. Zhang, F. Wang, X. Wei, Y. Yang, S. Xu, D. Deng and Y.-Z. Wang, From trash to treasure: Chemical recycling and upcycling of commodity plastic waste to fuels, high-valued chemicals and advanced materials, *J. Energy Chem.*, 2022, **69**, 369–388.

9 Q. Hou, M. Zhen, H. Qian, Y. Nie, X. Bai, T. Xia, M. Laiq Ur Rehman, Q. Li and M. Ju, Upcycling and catalytic degradation of plastic wastes, *Cell Rep. Phys. Sci.*, 2021, **2**, 100514.

10 W. T. Lee, A. van Muyden, F. D. Bobbink, M. D. Mensi, J. R. Carullo and P. J. Dyson, Mechanistic classification and benchmarking of polyolefin depolymerization over silica-alumina-based catalysts, *Nat. Commun.*, 2022, **13**, 4850.

11 A. Tennakoon, X. Wu, A. L. Paterson, S. Patnaik, Y. Pei, A. M. LaPointe, S. C. Ammal, R. A. Hackler, A. Heyden, I. I. Slowing, G. W. Coates, M. Delferro, B. Peters, W. Huang, A. D. Sadow and F. A. Perras, Catalytic upcycling of high-density polyethylene *via* a processive mechanism, *Nat. Catal.*, 2020, **3**, 893–901.

12 I. L. Peczak, R. M. Kennedy, R. A. Hackler, B. Lee, M. Meirow, E. Luijten, K. R. Poeppelmeier and M. Delferro, Treasuring trash: Pt/$SrTiO_3$ catalysts process plastic waste into high-value materials, *Matter*, 2023, **6**, 3296–3321.

13 L. D. Ellis, N. A. Rorrer, K. P. Sullivan, M. Otto, J. E. McGeehan, Y. Román-Leshkov, N. Wierckx and G. T. Beckham, Chemical and biological catalysis for plastics recycling and upcycling, *Nat. Catal.*, 2021, **4**, 539–556.

14 X. Zhang, M. Fevre, G. O. Jones and R. M. Waymouth, Catalysis as an Enabling Science for Sustainable Polymers, *Chem. Rev.*, 2018, **118**, 839–885.

15 R. Esquer and J. J. García, Metal-catalysed poly(ethylene) terephthalate and polyurethane degradations by glycolysis, *J. Organomet. Chem.*, 2019, **902**, 120972.

16 F. R. Veregue, C. T. Pereira da Silva, M. P. Moisés, J. G. Meneguin, M. R. Guilherme, P. A. Arroyo, S. L. Favaro, E. Radovanovic, E. M. Girotto and A. W. Rinaldi, Ultrasmall Cobalt Nanoparticles as a Catalyst for PET Glycolysis: A Green Protocol for Pure Hydroxyethyl Terephthalate Precipitation without Water, *ACS Sustainable Chem. Eng.*, 2018, **6**, 12017–12024.

17 L. Wursthorn, K. Beckett, J. O. Rothbaum, R. M. Cywar, C. Lincoln, Y. Kratish and T. J. Marks, Selective Lanthanide-Organic Catalyzed Depolymerization of Nylon-6 to ε-Caprolactam, *Angew. Chem., Int. Ed.*, 2022, **62**, e202212543.

18 A. Kumar, N. von Wolff, M. Rauch, Y.-Q. Zou, G. Shmul, Y. Ben-David, G. Leitus, L. Avram and D. Milstein, Hydrogenative Depolymerization of Nylons, *J. Am. Chem. Soc.*, 2020, **142**, 14267–14275.

19 M. A. M. E. Vertommen, V. A. Nierstrasz, M. v. d. Veer and M. M. C. G. Warmoeskerken, Enzymatic surface modification of poly(ethylene terephthalate), *J. Biotechnol.*, 2005, **120**, 376–386.

20 K. Świderek, S. Velasco-Lozano, M. À. Galmés, I. Olazabal, H. Sardon, F. López-Gallego and V. Moliner, Mechanistic studies of a lipase unveil effect of pH on hydrolysis products of small PET modules, *Nat. Commun.*, 2023, **14**, 3556.

21 R.-J. Müller, H. Schrader, J. Profe, K. Dresler and W.-D. Deckwer, Enzymatic Degradation of Poly(ethylene terephthalate): Rapid Hydrolyse using a Hydrolase from T. fusca, *Macromol. Rapid Commun.*, 2005, **26**, 1400–1405.

22 Å. M. Ronkvist, W. Xie, W. Lu and R. A. Gross, Cutinase-Catalyzed Hydrolysis of Poly(ethylene terephthalate), *Macromolecules*, 2009, **42**, 5128–5138.

23 A. M. de Castro, A. Carniel, J. Nicomedes Junior, A. da Conceicao Gomes and E. Valoni, Screening of commercial enzymes for poly(ethylene terephthalate) (PET) hydrolysis and synergy studies on different substrate sources, *J. Ind. Microbiol. Biotechnol.*, 2017, **44**, 835–844.

24 S. Yoshida, K. Hiraga, T. Takehana, I. Taniguchi, H. Yamaji, Y. Maeda, K. Toyohara, K. Miyamoto, Y. Kimura and K. Oda, A bacterium that degrades and assimilates poly(ethylene terephthalate), *Science*, 2016, **351**, 1196.

25 V. Tournier, C. M. Topham, A. Gilles, B. David, C. Folgoas, E. Moya-Leclair, E. Kamionka, M. L. Desrousseaux, H. Texier, S. Gavalda, M. Cot, E. Guemard, M. Dalibey, J. Nomme, G. Cioci, S. Barbe, M. Chateau, I. Andre, S. Duquesne and A. Marty, An engineered PET depolymerase to break down and recycle plastic bottles, *Nature*, 2020, **580**, 216–219.

26 H. Lu, D. J. Diaz, N. J. Czarnecki, C. Zhu, W. Kim, R. Shroff, D. J. Acosta, B. R. Alexander, H. O. Cole, Y. Zhang, N. A. Lynd, A. D. Ellington and H. S. Alper, Machine learning-aided engineering of hydrolases for PET depolymerization, *Nature*, 2022, **604**, 662–667.

27 R. Wei and W. Zimmermann, Microbial enzymes for the recycling of recalcitrant petroleum-based plastics: how far are we?, *Microb. Biotechnol.*, 2017, **10**, 1308–1322.

28 M. Santo, R. Weitsman and A. Sivan, The role of the copper-binding enzyme – laccase – in the biodegradation of polyethylene by the actinomycete Rhodococcus ruber, *Int. Biodeterior. Biodegrad.*, 2013, **84**, 204–210.

29 M. Fujisawa, H. Hirai and T. Nishida, Degradation of Polyethylene and Nylon-66 by the Laccase-Mediator System, *J. Polym. Environ.*, 2001, **9**, 103–108.

30 S. Ghatge, Y. Yang, J.-H. Ahn and H.-G. Hur, Biodegradation of polyethylene: a brief review, *Appl. Biol. Chem.*, 2020, **63**, 27.

31 M. Koutny, M. Sancelme, C. Dabin, N. Pichon, A.-M. Delort and J. Lemaire, Acquired biodegradability of polyethylenes containing pro-oxidant additives, *Polym. Degrad. Stab.*, 2006, **91**, 1495–1503.

32 A. Arkatkar, A. A. Juwarkar, S. Bhaduri, P. V. Uppara and M. Doble, Growth of Pseudomonas and Bacillus biofilms on pretreated polypropylene surface, *Int. Biodeterior. Biodegrad.*, 2010, **64**, 530–536.

33 H. J. Jeon and M. N. Kim, Functional analysis of alkane hydroxylase system derived from *Pseudomonas aeruginosa* E7 for low molecular weight polyethylene biodegradation, *Int. Biodeterior. Biodegrad.*, 2015, **103**, 141–146.

34 M. Yoon and H. Jeon, Biodegradation of Polyethylene by a Soil Bacterium and AlkB Cloned Recombinant Cell, *J. Biorem. Biodegrad.*, 2012, **3**, 145.

35 K. Nakamiya, G. Sakasita, T. Ooi and S. Kinoshita, Enzymatic degradation of polystyrene by hydroquinone peroxidase of Azotobacter beijerinckii HM121, *J. Ferment. Bioeng.*, 1997, **84**, 480–482.

36 V. Tournier, S. Duquesne, F. Guillamot, H. Cramail, D. Taton, A. Marty and I. André, Enzymes' Power for Plastics Degradation, *Chem. Rev.*, 2023, **123**, 5612–5701.

37 M. Parvinzadeh, R. Assefipour and A. Kiumarsi, Biohydrolysis of nylon 6,6 fiber with different proteolytic enzymes, *Polym. Degrad. Stab.*, 2009, **94**, 1197–1205.

38 C. Silva, R. Araújo, M. Casal, G. M. Gübitz and A. Cavaco-Paulo, Influence of mechanical agitation on cutinases and protease activity towards polyamide substrates, *Enzyme Microb. Technol.*, 2007, **40**, 1678–1685.

39 M. Kanelli, S. Vasilakos, S. Ladas, E. Symianakis, P. Christakopoulos and E. Topakas, Surface modification of polyamide 6.6 fibers by enzymatic hydrolysis, *Process Biochem.*, 2017, **59**, 97–103.

40 M. Fujisawa, H. Hirai and T. Nishida, Degradation of Polyethylene and Nylon-66 by the Laccase-Mediator System, *J. Polym. Environ.*, 2001, **9**, 103–108.

41 Y. Lee and N. K. Devaraj, Lipase mimetic cyclodextrins, *Chem. Sci.*, 2021, **12**, 1090–1094.

42 G. W. Gokel, S. Negin and R. Cantwell, in *Comprehensive Supramolecular Chemistry II*, ed. J. L. Atwood, Elsevier, Oxford, 2017, pp. 3–48, DOI: **10.1016/B978-0-12-409547-2.12519-3**.

43 M. M. Pereira, L. D. Dias and M. J. F. Calvete, Metalloporphyrins: Bioinspired Oxidation Catalysts, *ACS Catal.*, 2018, **8**, 10784–10808.

44 R. Tian, Y. Li, J. Xu, C. Hou, Q. Luo and J. Liu, Recent development in the design of artificial enzymes through molecular imprinting technology, *J. Mater. Chem. B*, 2022, **10**, 6590–6606.

45 J. Li, M. Zhu, M. Wang, W. Qi, R. Su and Z. He, Molecularly imprinted peptide-based enzyme mimics with enhanced activity and specificity, *Soft Matter*, 2020, **16**, 7033–7039.

46 Z. Yu, R. Lou, W. Pan, N. Li and B. Tang, Nanoenzymes in disease diagnosis and therapy, *Chem. Commun.*, 2020, **56**, 15513–15524.

47 S. Li, Z. Zhou, Z. Tie, B. Wang, M. Ye, L. Du, R. Cui, W. Liu, C. Wan, Q. Liu, S. Zhao, Q. Wang, Y. Zhang, S. Zhang, H. Zhang, Y. Du and H. Wei, Data-informed discovery of hydrolytic nanozymes, *Nat. Commun.*, 2022, **13**, 827.

48 B. Li, R. Ma, L. Chen, C. Zhou, Y.-X. Zhang, X. Wang, H. Huang, Q. Hu, X. Zheng, J. Yang, M. Shao, P. Hao, Y. Wu, Y. Che, C. Li, T. Qin, L. Gao, Z. Niu and Y. Li, Diatomic iron nanozyme with lipoxidase-like activity for efficient inactivation of enveloped virus, *Nat. Commun.*, 2023, **14**, 7312.

49 E. Ghanem and F. M. Raushel, in *eLS*, 2012, DOI: **10.1002/9780470015902.a0000714.pub2**.

50 C. Selvaraj, O. Rudhra, A. S. Alothaim, M. Alkhanani and S. K. Singh, in *Advances in Protein Chemistry and Structural Biology*, ed. R. Donev, Academic Press, 2022, vol. 130, pp. 59–83.

51 F. Yabukarski, J. T. Biel, M. M. Pinney, T. Doukov, A. S. Powers, J. S. Fraser and D. Herschlag, Assessment of enzyme active site positioning and tests of catalytic mechanisms through X-ray-derived conformational ensembles, *Proc. Natl. Acad. Sci. U. S. A.*, 2020, **117**, 33204–33215.

52 B. C. Knott, E. Erickson, M. D. Allen, J. E. Gado, R. Graham, F. L. Kearns, I. Pardo, E. Topuzlu, J. J. Anderson, H. P. Austin, G. Dominick, C. W. Johnson, N. A. Rorrer, C. J. Szostkiewicz, V. Copié, C. M. Payne, H. L. Woodcock, B. S. Donohoe, G. T. Beckham and J. E. McGeehan, Characterization and engineering of a two-enzyme system for plastics depolymerization, *Proc. Natl. Acad. Sci. U. S. A.*, 2020, **117**, 25476–25485.

53 H. P. Austin, M. D. Allen, B. S. Donohoe, N. A. Rorrer, F. L. Kearns, R. L. Silveira, B. C. Pollard, G. Dominick, R. Duman, K. El Omari, V. Mykhaylyk, A. Wagner, W. E. Michener, A. Amore, M. S. Skaf, M. F. Crowley, A. W. Thorne, C. W. Johnson, H. L. Woodcock, J. E. McGeehan and G. T. Beckham, Characterization and engineering of a plastic-degrading aromatic polyesterase, *Proc. Natl. Acad. Sci. U. S. A.*, 2018, **115**, E4350–E4357.

54 H. Hong, D. Ki, H. Seo, J. Park, J. Jang and K.-J. Kim, Discovery and rational engineering of PET hydrolase with both mesophilic and thermophilic PET hydrolase properties, *Nat. Commun.*, 2023, **14**, 4556.

55 X. Han, W. Liu, J. W. Huang, J. Ma, Y. Zheng, T. P. Ko, L. Xu, Y. S. Cheng, C. C. Chen and R. T. Guo, Structural insight into catalytic mechanism of PET hydrolase, *Nat. Commun.*, 2017, **8**, 2106.

56 M. Raynal, P. Ballester, A. Vidal-Ferran and P. W. N. M. van Leeuwen, Supramolecular catalysis. Part 2: artificial enzyme mimics, *Chem. Soc. Rev.*, 2014, **43**, 1734–1787.

57 A. Silakov, M. T. Olsen, S. Sproules, E. J. Reijerse, T. B. Rauchfuss and W. Lubitz, EPR/ENDOR, Mossbauer, and quantum-chemical investigations of diiron complexes mimicking the active oxidized state of [FeFe]hydrogenase, *Inorg. Chem.*, 2012, **51**, 8617–8628.

58 C. J. Allpress, K. Grubel, E. Szajna-Fuller, A. M. Arif and L. M. Berreau, Regioselective aliphatic carbon-carbon bond cleavage by a model system of relevance to iron-containing acireductone dioxygenase, *J. Am. Chem. Soc.*, 2013, **135**, 659–668.

59 S. Zheng, T. C. Berto, E. W. Dahl, M. B. Hoffman, A. L. Speelman and N. Lehnert, The functional model complex $[Fe_2(BPMP)(OPr)(NO)_2](BPh_4)_2$ provides insight into the mechanism of flavodiiron NO reductases, *J. Am. Chem. Soc.*, 2013, **135**, 4902–4905.

60 M. Zhao, H.-B. Wang, L.-N. Ji and Z.-W. Mao, Insights into metalloenzyme microenvironments: biomimetic metal complexes with a functional second coordination sphere, *Chem. Soc. Rev.*, 2013, **42**, 8360–8375.

61 F. Mancin, P. Scrimin and P. Tecilla, Progress in artificial metallonucleases, *Chem. Commun.*, 2012, **48**, 5545–5559.

62 M. D. Nothling, Z. Xiao, A. Bhaskaran, M. T. Blyth, C. W. Bennett, M. L. Coote and L. A. Connal, Synthetic Catalysts Inspired by Hydrolytic Enzymes, *ACS Catal.*, 2018, **9**, 168–187.

63 J. Bjerre, C. Rousseau, L. Marinescu and M. Bols, Artificial enzymes, "chemzymes": current state and perspectives, *Appl. Microbiol. Biotechnol.*, 2008, **81**, 1–11.

64 X. Li, Y. Zhou, Z. Lu, R. Shan, D. Sun, J. Li and P. Li, Switchable enzyme mimics based on self-assembled peptides for polyethylene terephthalate degradation, *J. Colloid Interface Sci.*, 2023, **646**, 198–208.

65 S. Zhang, Q. Hu, Y.-X. Zhang, H. Guo, Y. Wu, M. Sun, X. Zhu, J. Zhang, S. Gong, P. Liu and Z. Niu, Depolymerization of polyesters by a binuclear catalyst for plastic recycling, *Nat. Sustain.*, 2023, **6**, 965–973.

66 S. Zhang, Y. Xue, Y. Wu, Y.-X. Zhang, T. Tan and Z. Niu, PET recycling under mild conditions *via* substituent-modulated intramolecular hydrolysis, *Chem. Sci.*, 2023, **14**, 6558–6563.

67 G. Schenk, N. Mitic, L. R. Gahan, D. L. Ollis, R. P. McGeary and L. W. Guddat, Binuclear metallohydrolases: complex mechanistic strategies for a simple chemical reaction, *Acc. Chem. Res.*, 2012, **45**, 1593–1603.

68 J. S. Luterbacher, D. Martin Alonso and J. A. Dumesic, Targeted chemical upgrading of lignocellulosic biomass to platform molecules, *Green Chem.*, 2014, **16**, 4816–4838.

69 D. L. Zechel and S. G. Withers, Glycosidase mechanisms: anatomy of a finely tuned catalyst, *Acc. Chem. Res.*, 2000, **33**, 11–18.

70 S. Pengthaisong, B. Piniello, G. J. Davies, C. Rovira and J. R. Ketudat Cairns, Reaction Mechanism of Glycoside Hydrolase Family 116 Utilizes Perpendicular Protonation, *ACS Catal.*, 2023, **13**, 5850–5863.

71 J. F. Wardman, R. K. Bains, P. Rahfeld and S. G. Withers, Carbohydrate-active enzymes (CAZymes) in the gut microbiome, *Nat. Rev. Microbiol.*, 2022, **20**, 542–556.

72 M. Zangiabadi and Y. Zhao, Synergistic Hydrolysis of Cellulose by a Blend of Cellulase-Mimicking Polymeric Nanoparticle Catalysts, *J. Am. Chem. Soc.*, 2022, **144**, 17110–17119.

73 A. Shrotri, H. Kobayashi and A. Fukuoka, Air Oxidation of Activated Carbon to Synthesize a Biomimetic Catalyst for Hydrolysis of Cellulose, *ChemSusChem*, 2016, **9**, 1299–1303.

74 Z. Chen, Q. Li, Y. Xiao, C. Zhang, Z. Fu, Y. Liu, X. Yi, A. Zheng, C. Li and D. Yin, Acid–base synergistic catalysis of biochar sulfonic acid bearing polyamide for microwave-assisted hydrolysis of cellulose in water, *Cellulose*, 2018, **26**, 751–762.

75 E. J. Cho, S. J. Lee, K. Lee, D.-S. Lee, Y. J. Lee and H.-J. Bae, A Reusable Biomimetic Magnetic Nanoenzyme for Cellulosic Biomass Degradation, *BioEnergy Res.*, 2014, **8**, 788–795.
76 E. J. Cho, Y. Song, Y. J. Lee and H.-J. Bae, Preparation and characterization of novel green magnetic nanocatalyst for cellulosic biomass degradation under mild conditions, *J. Ind. Eng. Chem.*, 2016, **40**, 185–190.
77 H. Kobayashi, M. Yabushita, J.-y. Hasegawa and A. Fukuoka, Synergy of Vicinal Oxygenated Groups of Catalysts for Hydrolysis of Cellulosic Molecules, *J. Phys. Chem. C*, 2015, **119**, 20993–20999.
78 F. Yu, M. Smet, W. Dehaen and B. F. Sels, Water-soluble sulfonated hyperbranched poly(arylene oxindole) catalysts as functional biomimics of cellulases, *Chem. Commun.*, 2016, **52**, 2756–2759.
79 G. Yang, X. Luo and L. Shuai, Bioinspired Cellulase-Mimetic Solid Acid Catalysts for Cellulose Hydrolysis, *Front. Bioeng. Biotechnol.*, 2021, **9**, 770027.
80 F. Shen, R. L. Smith, L. Li, L. Yan and X. Qi, Eco-friendly Method for Efficient Conversion of Cellulose into Levulinic Acid in Pure Water with Cellulase-Mimetic Solid Acid Catalyst, *ACS Sustainable Chem. Eng.*, 2017, **5**, 2421–2427.
81 H.-X. Li, X. Zhang, Q. Wang, D. Yang, Q. Cao and L. Jin, Study on the hydrolysis of cellulose with the regenerable and recyclable multifunctional solid acid as a catalyst and its catalytic hydrolytic kinetics, *Cellulose*, 2019, **27**, 285–300.
82 C. Zhang, Z. Fu, Y. C. Liu, B. Dai, Y. Zou, X. Gong, Y. Wang, X. Deng, H. Wu, Q. Xu, K. R. Steven and D. Yin, Ionic liquid-functionalized biochar sulfonic acid as a biomimetic catalyst for hydrolysis of cellulose and bamboo under microwave irradiation, *Green Chem.*, 2012, **14**, 1928–1934.
83 Q. Yang and X. Pan, Bifunctional Porous Polymers Bearing Boronic and Sulfonic Acids for Hydrolysis of Cellulose, *ACS Sustainable Chem. Eng.*, 2016, **4**, 4824–4830.
84 T. Deguchi, M. Kakezawa and T. Nishida, Nylon biodegradation by lignin-degrading fungi, *Appl. Environ. Microbiol.*, 1997, **63**, 329–331.
85 T. Deguchi, Y. Kitaoka, M. Kakezawa and T. Nishida, Purification and characterization of a nylon-degrading enzyme, *Appl. Environ. Microbiol.*, 1998, **64**, 1366–1371.
86 A. Nyyssölä and J. Ahlgren, Microbial degradation of polyacrylamide and the deamination product polyacrylate, *Int. Biodeterior. Biodegrad.*, 2019, **139**, 24–33.
87 K. Nakamiya, T. Ooi and S. Kinoshita, Degradation of synthetic water-soluble polymers by hydroquinone peroxidase, *J. Ferment. Bioeng.*, 1997, **84**, 213–218.
88 W. J. R. Gilbert, S. J. Johnson, J. S. Tsau, J. T. Liang and A. M. Scurto, Enzymatic degradation of polyacrylamide in aqueous solution with peroxidase and H_2O_2, *J. Appl. Polym. Sci.*, 2016, **134**, 44560.
89 W. Bankeeree, C. Samathayanon, S. Prasongsuk, P. Lotrakul and S. Kiatkamjornwong, Rapid Degradation of Superabsorbent Poly(Potassium Acrylate) and its Acrylamide Copolymer *Via* Thermo-Oxidation by Hydrogen Peroxide, *J. Polym. Environ.*, 2021, **29**, 3964–3976.
90 T. L. Poulos, Heme Enzyme Structure and Function, *Chem. Rev.*, 2014, **114**, 3919–3962.
91 C. Zhu, W. Ding, T. Shen, C. Tang, C. Sun, S. Xu, Y. Chen, J. Wu and H. Ying, Metallo-deuteroporphyrin as a biomimetic catalyst for the catalytic oxidation of lignin to aromatics, *ChemSusChem*, 2015, **8**, 1768–1778.
92 T. Jian, Y. Zhou, P. Wang, W. Yang, P. Mu, X. Zhang, X. Zhang and C. L. Chen, Highly stable and tunable peptoid/hemin enzymatic mimetics with natural peroxidase-like activities, *Nat. Commun.*, 2022, **13**, 3025.
93 N. Zhu, C. Liu, R. Liu, X. Niu, D. Xiong, K. Wang, D. Yin and Z. Zhang, Biomimic Nanozymes with Tunable Peroxidase-like Activity Based on the Confinement Effect of Metal–Organic Frameworks (MOFs) for Biosensing, *Anal. Chem.*, 2022, **94**, 4821–4830.
94 F.-X. Qin, S.-Y. Jia, F.-F. Wang, S.-H. Wu, J. Song and Y. Liu, Hemin@metal–organic framework with peroxidase-like activity and its application to glucose detection, *Catal. Sci. Technol.*, 2013, **3**, 2761–2768.
95 Q. Xin, X. Jia, A. Nawaz, W. Xie, L. Li and J. R. Gong, Mimicking peroxidase active site microenvironment by functionalized graphene quantum dots, *Nano Res.*, 2020, **13**, 1427–1433.
96 M. A. Castriciano, A. Romeo, M. C. Baratto, R. Pogni and L. M. Scolaro, Supramolecular mimetic peroxidase based on hemin and PAMAM dendrimers, *Chem. Commun.*, 2008, **6**, 688–690.
97 J. Wu, X. Wang, Q. Wang, Z. Lou, S. Li, Y. Zhu, L. Qin and H. Wei, Nanomaterials with enzyme-like characteristics (nanozymes): next-generation artificial enzymes (II), *Chem. Soc. Rev.*, 2019, **48**, 1004–1076.
98 Q. Diao, X. Chen, Z. Tang, S. Li, Q. Tian, Z. Bu, H. Liu, J. Liu and X. Niu, Nanozymes: powerful catalytic materials for environmental pollutant detection and degradation, *Environ. Sci.: Nano*, 2024, **11**, 766–796.
99 L. Gao, J. Zhuang, L. Nie, J. Zhang, Y. Zhang, N. Gu, T. Wang, J. Feng, D. Yang, S. Perrett and X. Yan, Intrinsic peroxidase-like activity of ferromagnetic nanoparticles, *Nat. Nanotechnol.*, 2007, **2**, 577–583.
100 K. Fan, H. Wang, J. Xi, Q. Liu, X. Meng, D. Duan, L. Gao and X. Yan, Optimization of Fe_3O_4 nanozyme activity *via* single amino acid modification mimicking an enzyme active site, *Chem. Commun.*, 2017, **53**, 424–427.
101 M. Liang, K. Fan, Y. Pan, H. Jiang, F. Wang, D. Yang, D. Lu, J. Feng, J. Zhao, L. Yang and X. Yan, Fe_3O_4 Magnetic Nanoparticle Peroxidase Mimetic-Based Colorimetric Assay for the Rapid Detection of Organophosphorus Pesticide and Nerve Agent, *Anal. Chem.*, 2013, **85**, 308–312.
102 M. Zandieh and J. Liu, Removal and Degradation of Microplastics Using the Magnetic and Nanozyme Activities of Bare Iron Oxide Nanoaggregates, *Angew. Chem., Int. Ed.*, 2022, **61**, e202212013.
103 N. Mitić, S. J. Smith, A. Neves, L. W. Guddat, L. R. Gahan and G. Schenk, The Catalytic Mechanisms of Binuclear Metallohydrolases, *Chem. Rev.*, 2006, **106**, 3338–3363.
104 Y.-W. Lin, Rational design of metalloenzymes: From single to multiple active sites, *Coord. Chem. Rev.*, 2017, **336**, 1–27.

105 J. D. McCarter and G. Stephen Withers, Mechanisms of enzymatic glycoside hydrolysis, *Curr. Opin. Struct. Biol.*, 1994, **4**, 885–892.
106 J. N. H. Reek, B. De Bruin, S. Pullen, T. J. Mooibroek, A. M. Kluwer and X. Caumes, Transition Metal Catalysis Controlled by Hydrogen Bonding in the Second Coordination Sphere, *Chem. Rev.*, 2022, **122**, 12308–12369.
107 T. Klabunde, H. Witzel and B. Krebs, Mechanism of Fe(III)–Zn(II) Purple Acid Phosphatase Based on Crystal Structures, *J. Mol. Biol.*, 1996, **259**, 737–748.
108 H. Kaija, S. L. Alatalo, J. M. Halleen, Y. Lindqvist, G. Schneider, H. Kalervo Väänänen and P. Vihko, Phosphatase and Oxygen Radical-Generating Activities of Mammalian Purple Acid Phosphatase Are Functionally Independent, *Biochem. Biophys. Res. Commun.*, 2002, **292**, 128–132.
109 Y. An, M.-L. Tong, L.-N. Ji and Z.-W. Mao, Double-strand DNA cleavage by copper complexes of 2,2′-dipyridyl with electropositive pendants, *Dalton Trans.*, 2006, 2066–2071.
110 L. Tjioe, A. Meininger, T. Joshi, L. Spiccia and B. Graham, Efficient Plasmid DNA Cleavage by Copper(II) Complexes of 1,4,7-Triazacyclononane Ligands Featuring Xylyl-Linked Guanidinium Groups, *Inorg. Chem.*, 2011, **50**, 4327–4339.
111 B. De Souza, G. L. Kreft, T. Bortolotto, H. Terenzi, A. J. Bortoluzzi, E. E. Castellano, R. A. Peralta, J. B. Domingos and A. Neves, Second-Coordination-Sphere Effects Increase the Catalytic Efficiency of an Extended Model for $Fe^{III}M^{II}$ Purple Acid Phosphatases, *Inorg. Chem.*, 2013, **52**, 3594–3596.
112 G. A. D. S. Silva, A. L. Amorim, B. D. Souza, P. Gabriel, H. Terenzi, E. Nordlander, A. Neves and R. A. Peralta, Synthesis and characterization of $Fe^{III}(\mu\text{-}OH)Zn^{II}$ complexes: effects of a second coordination sphere and increase in the chelate ring size on the hydrolysis of a phosphate diester and DNA, *Dalton Trans.*, 2017, **46**, 11380–11394.
113 T. P. Camargo, A. Neves, R. A. Peralta, C. Chaves, E. C. P. Maia, E. H. Lizarazo-Jaimes, D. A. Gomes, T. Bortolotto, D. R. Norberto, H. Terenzi, D. L. Tierney and G. Schenk, Second-Sphere Effects in Dinuclear $Fe^{III}Zn^{II}$ Hydrolase Biomimetics: Tuning Binding and Reactivity Properties, *Inorg. Chem.*, 2018, **57**, 187–203.
114 M. Borkowska, M. Siek, D. V. Kolygina, Y. I. Sobolev, S. Lach, S. Kumar, Y.-K. Cho, K. Kandere-Grzybowska and B. A. Grzybowski, Targeted crystallization of mixed-charge nanoparticles in lysosomes induces selective death of cancer cells, *Nat. Nanotechnol.*, 2020, **15**, 331–341.
115 C. Zhang, P. Gotico, R. Guillot, D. Dragoe, W. Leibl, Z. Halime and A. Aukauloo, Bio-Inspired Bimetallic Cooperativity Through a Hydrogen Bonding Spacer in CO_2 Reduction, *Angew. Chem., Int. Ed.*, 2023, **62**, e202214665.
116 M. L. Helm, M. P. Stewart, R. M. Bullock, M. R. DuBois and D. L. DuBois, A Synthetic Nickel Electrocatalyst with a Turnover Frequency Above 100,000 s^{-1} for H_2 Production, *Science*, 2011, **333**, 863–866.
117 B. Sharma and S. Striegler, Tailored Interactions of the Secondary Coordination Sphere Enhance the Hydrolytic Activity of Cross-Linked Microgels, *ACS Catal.*, 2019, **9**, 1686–1691.
118 R. Suno, H. Niwa, D. Tsuchiya, X. Zhang, M. Yoshida and K. Morikawa, Structure of the whole cytosolic region of ATP-dependent protease FtsH, *Mol. Cell*, 2006, **22**, 575–585.
119 C. Divne, J. Ståhlberg, T. Reinikainen, L. Ruohonen, G. Pettersson, J. K. C. Knowles, T. T. Teeri and T. A. Jones, The Three-Dimensional Crystal Structure of the Catalytic Core of Cellobiohydrolase I from *Trichoderma reesei*, *Science*, 1994, **265**, 524–528.
120 R. L. Silveira and M. S. Skaf, Concerted motions and large-scale structural fluctuations of Trichoderma reesei Cel7A cellobiohydrolase, *Phys. Chem. Chem. Phys.*, 2018, **20**, 7498–7507.
121 S. Joo, I. J. Cho, H. Seo, H. F. Son, H.-Y. Sagong, T. J. Shin, S. Y. Choi, S. Y. Lee and K.-J. Kim, Structural insight into molecular mechanism of poly(ethylene terephthalate) degradation, *Nat. Commun.*, 2018, **9**, 382.
122 A. Mujahid and F. L. Dickert, in *Molecularly Imprinted Catalysts*, 2016, pp. 79–101, DOI: **10.1016/b978-0-12-801301-4.00005-0**.
123 X. Li, M. Zangiabadi and Y. Zhao, Molecularly Imprinted Synthetic Glucosidase for the Hydrolysis of Cellulose in Aqueous and Nonaqueous Solutions, *J. Am. Chem. Soc.*, 2021, **143**, 5172–5181.
124 Y. Yuan, Y. Yang, M. Faheem, X. Zou, X. Ma, Z. Wang, Q. Meng, L. Wang, S. Zhao and G. Zhu, Molecularly Imprinted Porous Aromatic Frameworks Serving as Porous Artificial Enzymes, *Adv. Mater.*, 2018, **30**, 1800069.
125 L. Wan, H. Liu, C. Huang and X. Shen, Enzyme-like MOFs: synthetic molecular receptors with high binding capacity and their application in selective photocatalysis, *J. Mater. Chem. A*, 2020, **8**, 25931–25940.
126 Z. Zhang, X. Zhang, B. Liu and J. Liu, Molecular Imprinting on Inorganic Nanozymes for Hundred-fold Enzyme Specificity, *J. Am. Chem. Soc.*, 2017, **139**, 5412–5419.
127 J. M. Duval, A. J. B. Kemperman, B. Folkers, M. H. V. Mulder, G. Desgrandchamps and C. A. Smolders, Preparation of zeolite filled glassy polymer membranes, *J. Appl. Polym. Sci.*, 1994, **54**, 409–418.
128 I. F. J. Vankelecom, E. Merckx, M. Luts and J. B. Uytterhoeven, Incorporation of Zeolites in Polyimide Membranes, *J. Phys. Chem.*, 1995, **99**, 13187–13192.
129 P. Duan, J. C. Moreton, S. R. Tavares, R. Semino, G. Maurin, S. M. Cohen and K. Schmidt-Rohr, Polymer Infiltration into Metal-Organic Frameworks in Mixed-Matrix Membranes Detected *in Situ* by NMR, *J. Am. Chem. Soc.*, 2019, **141**, 7589–7595.
130 X. Wu, A. Tennakoon, R. Yappert, M. Esveld, M. S. Ferrandon, R. A. Hackler, A. M. LaPointe, A. Heyden, M. Delferro, B. Peters, A. D. Sadow and W. Huang, Size-Controlled Nanoparticles Embedded in a Mesoporous Architecture Leading to Efficient and Selective Hydrogenolysis of Polyolefins, *J. Am. Chem. Soc.*, 2022, **144**, 5323–5334.

131 J. Duan, W. Chen, C. Wang, L. Wang, Z. Liu, X. Yi, W. Fang, H. Wang, H. Wei, S. Xu, Y. Yang, Q. Yang, Z. Bao, Z. Zhang, Q. Ren, H. Zhou, X. Qin, A. Zheng and F.-S. Xiao, Coking-Resistant Polyethylene Upcycling Modulated by Zeolite Micropore Diffusion, *J. Am. Chem. Soc.*, 2022, **144**, 14269–14277.

132 A. R. Riscoe, C. J. Wrasman, A. A. Herzing, A. S. Hoffman, A. Menon, A. Boubnov, M. Vargas, S. R. Bare and M. Cargnello, Transition state and product diffusion control by polymer–nanocrystal hybrid catalysts, *Nat. Catal.*, 2019, **2**, 852–863.

133 A. Tennakoon, X. Wu, M. Meirow, D. Howell, J. Willmon, J. Yu, J. V. Lamb, M. Delferro, E. Luijten, W. Huang and A. D. Sadow, Two Mesoporous Domains Are Better Than One for Catalytic Deconstruction of Polyolefins, *J. Am. Chem. Soc.*, 2023, **145**, 17936–17944.

134 W. Zhao, S. Hasegawa, J. Fujita, F. Yoshii, T. Sasaki, K. Makuuchi, J. Sun and S.-i. Nishimoto, Effects of zeolites on the pyrolysis of polypropylene, *Polym. Degrad. Stab.*, 1996, **53**, 129–135.

135 T.-T. Wei, K.-J. Wu, S.-L. Lee and Y.-H. Lin, Chemical recycling of post-consumer polymer waste over fluidizing cracking catalysts for producing chemicals and hydrocarbon fuels, *Resour., Conserv. Recycl.*, 2010, **54**, 952–961.

136 J. Gancedo, H. Li, J. S. Walz, L. Faba, S. Ordoñez and G. W. Huber, Investigation into the shape selectivity of zeolites for conversion of polyolefin plastic pyrolysis oil model compound, *Appl. Catal., A*, 2024, **669**, 119484.

137 Y. Nakaji, M. Tamura, S. Miyaoka, S. Kumagai, M. Tanji, Y. Nakagawa, T. Yoshioka and K. Tomishige, Low-temperature catalytic upgrading of waste polyolefinic plastics into liquid fuels and waxes, *Appl. Catal., B*, 2021, **285**, 119805.

138 S. Liu, P. A. Kots, B. C. Vance, A. Danielson and D. G. Vlachos, Plastic waste to fuels by hydrocracking at mild conditions, *Sci. Adv.*, 2021, **7**, eabf8283.

139 R. Lin, B. Villacorta Hernandez, L. Ge and Z. Zhu, Metal organic framework based mixed matrix membranes: an overview on filler/polymer interfaces, *J. Mater. Chem. A*, 2018, **6**, 293–312.

140 Y. Wu, J. Tian, M. Sun, L. Gao, J. Xu and Z. Niu, Embedding an esterase mimic inside polyesters to realize rapid and complete degradation without compromising their utility, *Green Chem.*, 2024, **26**(5), 2851–2857.